UNIVERSITÀ DEGLI STUDI DI PADOVA
DIPARTIMENTO DI INGEGNERIA INDUSTRIALE
DIPARTIMENTO DI INGEGNERIA CIVILE, EDILE E AMBIENTALE

CORSO DI LAUREA MAGISTRALE IN INGEGNERIA DELLA SICUREZZA CIVILE E INDUSTRIALE

TESI DI LAUREA

Improvement of soil thermo-hydro-mechanical properties with deep mixing technique and its effect in geotechnical stability problems

Relatore:
Prof. Paolo Simonini
Prof. Anne-Lise Beaucour

Laureanda:
Sara ZANARDI

ANNO ACCADEMICO 2019-2020

Abstract

I did my internship at the University of Cergy Paris for a six-month period. During this internship I have collaborated on a research study on soil concrete. The approach tested in the laboratory L2MGC of the university consists in studying different mixtures of soil-cement composed of natural soil taken from a construction site (Esbly) and CEM III/C cement with a constant W/C ratio.

Contents

List of Figures

List of Tables

Chapter 1

Bibliographical study

1.1 Introduction

Soil improvement in its broadest sense is the alteration of any property of a soil to improve its engineering performance such as strength, reduced compressibility, reduced permeability, or improved ground water condition. This may be either a temporary process to permit the construction of a facility or may be a permanent measure to improve the performance of the completed facility. There are various techniques used for the improvement of the soil based on the construction activity and type of soil.

The Deep Soil Mixing Method (DMM) was invented in Japan and Scandinavia. Its use is growing across the world in strengthening and sealing weak and permeable ground. The method helps to achieve significant improvement of mechanical and physical properties of the existing soil, which after mixing with cement or compound binders becomes the so-called soil-mix (or soil-cement). The stabilised soil material that is produced generally has a higher strength, lower permeability and lower compressibility than the native soil. Although the DMM technology is based on simple principles it requires, on the one hand, having significant experience and expertise in associated planning stages, involving soil-mix geotechnical design and execution. On the other hand, it also requires the use of specialised rigs and mixing tools to meet specifications imposed by ongoing quality assessments and performance monitoring procedures. Advantages of DMM technology is based on a stimulating concept of improving natural soils to match adopted design requirements, so eliminating problematic excavation and replacement or more expensive deep foundation methods. Wide application range and variable patterns of execution of soil mixing columns allow for obtaining safe and very economic ground engineering solutions.

1.2 Deep Soil Mixing

The deep mixing method is a deep in-situ admixture stabilization technique using lime, cement or lime-based and cement-based special binders. Compared to the other ground improvement techniques deep mixing has advantages such as the large strength increase within a month period, little adverse impact on environment and high applicability to any kind of soil if binder type and amount are properly selected. The application covers on-land and in-water constructions ranging from strengthening the foundation ground of buildings, embankment supports, earth retaining structures, retrofit and renovation of urban infrastructures, liquefaction hazards mitigation, man-made island constructions and seepage control. Some examples are described in the following table.

Application	**Description**
Embankment support (both new embankments and embankment widening)	Embankement supported on isolated DMM elements (single columns, multi-auger overlapping columns, or barrettes), continous shear walls formed by overlapping elements, or fully treated blocks formed by overlapping elements
Culvert through an embankment on DMM	Cut and cover culvert supported on DMM through an embankment supported on DMM
Bridge abutment support	Abutment and embankment supported on deep foundations and embankment on DMM
Retaining wall foundations	Retaining wall supported on DMM without retained soil supported on DMM
Bridge pier support	Bridge pier supported on DMM; generally, DMM would be used for this application if DMM is also being used to support the bridge approaches

Table 1.1: Use of DMM for embankment and foundation applications [1]

Applicabile soil type The system is most applicable in soft soils. Boulders and other obstructions can be a problem. Cohesionless soils are easier to mix than cohesive soils. The ease of mixing cohesive soils varies inversely with plasticity and proportionally with moisture content. The system is most commonly used

in soft cohesive soils as other soils can often be treated more economically with other technologies. Organic soils are problematic and generally require much larger cement content.

Equipment A high-volume batching system is required to maintain productivity and economics. The components consist of an accurately controlled mixer, temporary storage and high-volume pumps. A drilling system is required to turn the mixing tool in the ground. It can be a single- or multiple-axis tool. Tool designs vary with soil types and are often custom-built for specific projects.

Procedure The binder is injected as the tool is advanced down to assist in penetration and to take advantage of this initial mixing. The soil and binder are mixed a second time as the tool is extracted. The rate of penetration and extraction is controlled to achieve adequate mixing. Single columns or integrated walls are created as the augers are worked in overlapping configurations. Treatment depths as great as 31 meters have been achieved.

Materials For wet soil mixing, the binder is delivered in a slurry form. Slurry volumes range from 20 to 40% of the soul volume being mixed. Common binders are Portland cement, fly ash, ground blast furnace slag, and additives. For dry soil mixing, the same materials (also line) are pumped dry using compressed air. Preproduction laboratory testing is used to determine mix energy and grout proportions.

Design Unconfined compressive strength and permeability are generally the design parameters. A standard analysis is performed to determine the required geometry based on the parameters achievable in the soil to be mixed. For excavation support walls, the mass can be designed as a standard excavation wall, or a thicker mass can be created and analyzed as a gravity structure, calculating the mass' shear, sliding and overturning, as well as the global stability of the system. When used as structural load bearing columns, a standard bearing capacity and settlement analysis is performed as would be for any cast in place pier. Anchored retention using steel reinforcement is common for support walls. [2]

1.2.1 Dry Soil Mixing

Dry soil mixing (Figure 1.1) is a low-vibration, quiet, clean form of ground treatment technique that is often used in very soft and wet soil conditions and has the advantage of producing very little spoil. The high speed rotating mixing tool is advanced to the maximum depth, "disturbing" the soil on the way down. The dry binder is then pumped with air through the hollow stem as the tool is rotated on extraction. It is very effective in soft clays and peats. Soils with moisture content, greater than 60% are most economically treated. This process uses cementicious binders to create bond among soil particles and thus increases the shear strength and reduces the compressibility of weak soils. The most commonly used binding agents are cement, lime, gypsum, or slag. Generally, the improvement in shear strength and compressibility increases with the binder dosage.

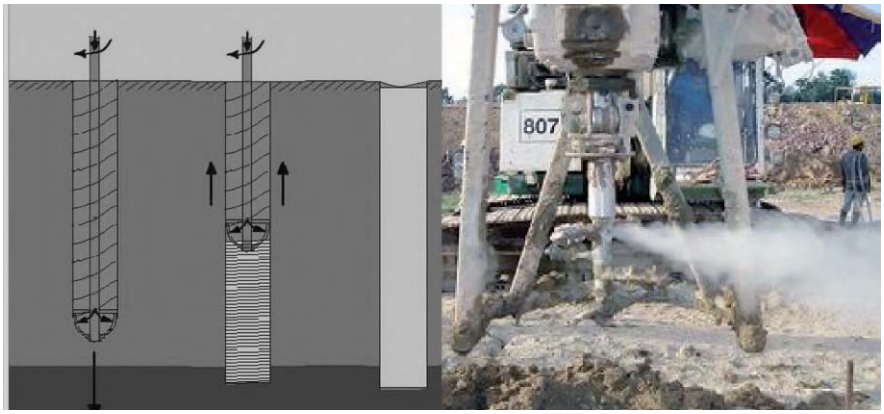

Figure 1.1: Illustration of dry soil mixing method and ejection of dry binder

1.2.2 Wet Soil Mixing

Wet soil mixing (Figure 1.2) is a similar technique except that a slurry binder is used making it more applicable with dryer soils (moisture contents less than 60%). The grout slurry is pumped through the hollow stem to the trailing edge of the mixing blades both during penetration and extraction.Depending on the in situ soils, the volume of grout slurry necessary varies from 20 to 40% of the soil volume. The technique produces a similar amount of spoil (20 to 40%) which is essentially excess mixed soil which, after setting up, can often be used as structural fill. The grout slurry can be composed of Portland cement, fly ash, and ground granulated blast furnace slag.

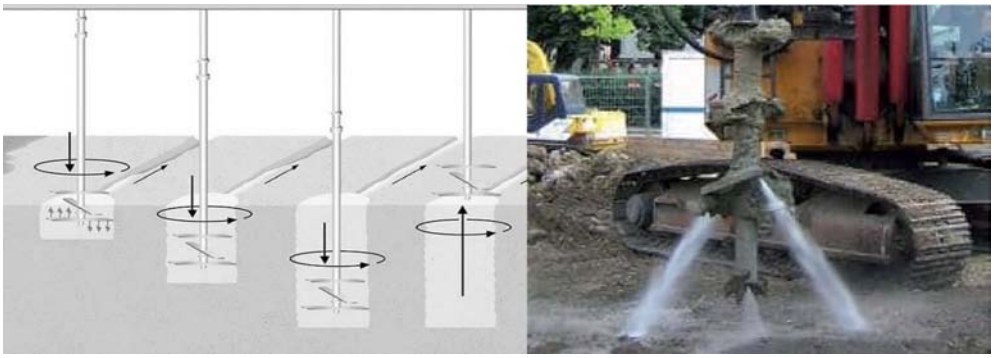

Figure 1.2: Illustration of wet soil mixing method and ejection of slurry

1.3 Properties of soil -binder mixture

Lime, cement and various by-product materials are used to modify and stabilize soils. Water content, types and graduation of soil, soil minerals, organic content, type and amount of stabilizer, in addition to curing conditions (time, temperature and moisture) represent the most important factors controlling the strength development.

1.3.1 Concrete

Concrete is a composite material, it's a conglomerate of stones, gravels, sand and cement, which, binding all together, become a hard and resistant product. The stone elements (called aggregates) and the cement (which is considered an hydraulic binder) are blended with water to form a liquid mixture which will be harden to form concrete. In addition to this material some other chemical components (called additives) could be add to modify some particular characteristics of concrete.

1.3.2 Cement

Among the hydraulic binder the most important component is certainly the cement, in particular Portland cement.It is available as a powder which, mixed with water with a ratio (W/C), produces a paste easily shaped and it starts to harden after some hours, losing its plasticity and, after some days, it develops compactness and rigidity. Cement comes from a fabrication process organized in mix design of raw materials, grinding and burning at about 1500 °C, obtaining clinker which is mixed with a small quantity (5%) of gypsum to adjust the cement hardening.

The principal components of Portland Cement are:

- Trialcium aluminate ($3CaO \cdot Al_2O_3$)
- Tricalcium silicate ($3CaO \cdot SiO_2$)
- Beta dicalcium silicate ($CaO \cdot SiO_2$)
- Tetracalcium alluminoferrite ($4CaO \cdot AlO3 \cdot Fe_2O_3$)

The minor components are usually:

- Magnesium oxide (MgO)
- Tricalcium ferrite ($3CaO \cdot Fe_2O_3$)
- Whilst gypsum ($CaSO_4 \cdot 2H_2O$)

Among the principal component of clinker, the silicates are in percentage of 80 %, while the aluminates has a content of 20 %, and they are responsible of setting processes. The silicates cause the hardening of paste.
The main types of cements produced correspond to and comply with European standards (AITEC):

- CEM I (Portland cement) and CEM II (Portland composite cement): these are the cements most commonly used in conventional reinforced-concrete structures as bridges, industrial and commercial buildings or housing. Some special formulations of these cements are also used in underground works in aggressive environments or under the sea.
- CEM III (blastfurnace cement): cements giving off low heat during hydration and with low sulfate contents, used for underground works in aggressive environments or for maritime works. Clinker until 65%.
- CEM IV (pozzolanic cements): cements using mineral ingredients of volcanic origin that display hydraulic properties
- CEM V (composite cement): cements using a mixture of clinker,blastfurnace slags and pozzolan.

1.3.3 Hydration process

Mixing cement and water initiates a chemical reaction known as hydration reaction. This process occurs rapidly and produces two types of primary cementitious materials: calcium-aluminate-hydrate (C-A-H) and calcium-silicate hydrate (C-S-H). These cemented products bind soil particles together and produce a strong and hard mixture with time.The reaction is exothermic.

Setting:

$$(3CaO \cdot Al_2O_3)_2 + (x+8)H_2O \rightarrow 4CaO \cdot Al_2O_3 \cdot xH_2O + 2CaO \cdot Al_2O_3 \cdot 8H_2O$$
$$3CaO \cdot Al_2O_3 + 12H_2O + Ca(OH)_2 \rightarrow 4CaO \cdot Al_2O_3 \cdot 13H_2O$$
$$4CaO \cdot Al_2O_3 \cdot Fe_2O_3 + 7H_2O \rightarrow 3CaO \cdot Al_2O_3 \cdot 6H_2O + CaO \cdot Fe_2O_3 \cdot H_2O$$

Hardening:

$$(3\ CaO \cdot SiO_2)_2 + (x+3)H_2O \rightarrow 3\ CaO2 \cdot SiO_2 \cdot xH_2O + 3\ Ca(OH)_2$$
$$(2\ CaO \cdot SiO_2)_2 + (x+1)H_2O \rightarrow 3\ CaO2 \cdot SiO_2 \cdot xH_2O + Ca(OH)_2$$

$Ca(OH)_2$ is called portlandite and it is almost the 20-25% of total solid volume. CSH is called gel, and it cover almost the 50-60% of solid volume in the cement paste.

The design strength of a cement-treated soil is usually determined based on its strength at 28days, in a manner similar to concrete but presents also a long-term strength. The large gap between the design strength at 28 days and the actual long-term strength beyond 28 days has both advantages and disadvantages in practice.The development of long-term strength serves to increase the stability of foundations and immobilize heavy metals; however, the development of excessive strength could prevent the re-excavation of the stabilized foundation. In general,as shown in Figure 1.3 [1], the mechanism of strength development of cement-treated soils is explained by a combination of the following:

- (1) The original strength of the cement-free soil;
- (2) Improvement in basic soil properties owing to the decrease in water content and ion exchange
- (3) Cement hydration

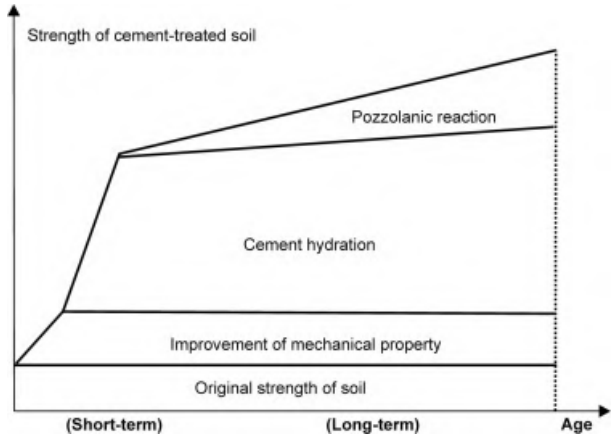

Figure 1.3: Typical explanation of mechanism of increase in strength of cement-treated soils

- (4) Pozzolanic reaction

While the short-term increase in the strength of cement-treated soils up to 28 days is mainly due to cement hydration, the long-term increase in the strength beyond 28 days is due to the pozzolanic reaction between soil and cement paste under the high-alkalinity conditions created by the cement.
In this study the cement used is the CEM III/C and contains 85 % blast furnace slags. Slags can replace partially clinker because it is a hydraulic binder and the reaction occurs with the OH^- available in the mixing water.
The pozzolanic reaction between Portlandite resulting from clinker hydration and silicon-aluminated products is the following :

$$Laitiers + Ca(OH)_2 \rightarrow C - S - H \tag{1.1}$$

The quantity of C-S-H produced in the case of CEM III/C is preponderant, while for ettringite is low. In this last process all Portlandite is consumed in C-S-H formation.
Normally aggregates contained in concrete are inert and they don't react with water or cement, while soil concrete mixtures may contain a variable fraction of clay inside, that present a strong interaction with water and also a strong chemical interaction with cement. During the formation of C-S-H and $CA(OH)_2$ a large amount of water is consumed and consequently the pH of the solution reaches approximately the value of 12.5. Strong bases (high pH) dissolve silicium and aluminium (acids) from clay minerals to form insoluble compounds, SiO_2 and Al_2O_3. These compounds react in their turn with the hydrated lime to form

C-S-H and C-A-H [11].These reactions are known as pozzolanic reactions:

$$Ca(OH)_2 + SiO_2 \rightarrow CSH$$
$$Ca(OH)_2 + Al_2O_3 \rightarrow CAH$$

The process is influenced by the initial state of saturation because only below a certain threshold the cationic exchange mechanisms occurs. Clays increase the setting time because of the fine particle size compared to cement particles.

1.4 Water role

Water and its ratio with cement (W/C) are one of the most important characteristics in concrete mix design. The water inside the concrete paste could be present in different forms, depending on the connection with cement paste:

- Free water included in pores with diameters superior at 50 nm (called macropores) and if it is removed there isn't a volume variation. It is called free because any attractive forces are present;
- Adsorbed water connected with cement paste by attraction forces, if this kind of water is lost, the phenomenon of shrinkage occurs; this type of water could be removed by concrete drying (if the humidity is less than 10%);
- Water chemically linked with hydration products, i.e. the water that is free to move when concrete is exposed to high temperature

The quality of water is important too , because the impurities in it may interfere with setting, with strength or something. Usually the water used during the mix has to be clear, without impurities.
In the case of cement-treated soil the ratio W/C is very important to determine the optimal amount of water in order to obtain the workability needed for placing in situ without compaction or vibration and for cement hydration process. The type of soil strongly influences this parameter too.

1.4.1 Soil type

The soil is the major component of soil-concrete mixtures and its physical and chemical properties can affect the final properties of the material. Parameters such as grain size curve,water content, water pH, Atterberg limits, type of clay and its cation exchange capacity are essential for the purpose of this study.

The table below shows the soil classification based on gran size, from clay ($< 2\mu$m) to rock boulder ($> 20cm$). In Deep Soil Mixing treated soils are generally clay, sand and silt but may contain also some gravel in small quantities.

Type		**Size (mm)**
Very coarse soils	Boulder size	> 300
	Cobble size	80 - 300
Coarse soils	Gravel size	4.75-80
	Sand size	0.075 - 4.75
Fine soils	Silt size	0.002 - 0.075
	Clay size	< 0.002

Table 1.2: Grain size

The compressive strength mostly increases in function of the grain size curve. In the figure 1.4 the distinction between sable and gravels, that are able to achieve higher values of compressive strength,are compared to cohesive soils as silt and clay.

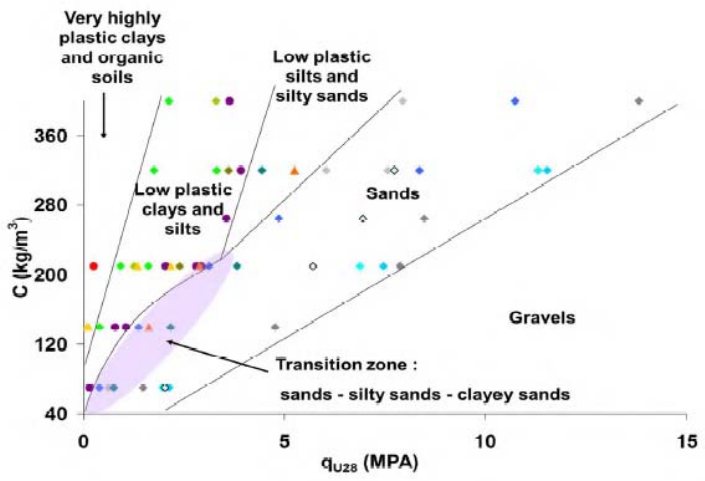

Figure 1.4: Nomograms linking cement content /compressive strength 28 [4]

Clay minerals

Clay minerals are commonly phyllosilicates or layer silicates.These minerals have platy morphology because of the arrangement of atoms in the structure. There

are two basic components to the structure: a sheet of corner-linked tetrahedra (Si^{4+} cations) and a sheet of edge-sharing octahedra (Al^{3+} cations) [3].
The minerals found in clay are generally silicates less than 2 microns in size. The small size of the particles and their unique crystal structures give clay materials special properties, including cation exchange capabilities, plastic behavior when wet, catalytic abilities, swelling behavior, and low permeabilities.
Clay minerals all have a great affinity for water, which molecules are strongly attracted to clay mineral surfaces. The process by which some clay minerals swell when they take up water is reversible. Swelling clay expands or contracts in response to changes in environmental factors (wet and dry conditions, temperature). Another important property of clay minerals is the ability to exchange ions (Cation Exchange Capacity), relates to the charged surface of clay minerals. Ions can be attracted to the surface of a clay particle or taken up within the structure of these minerals. The adsorption of clay is proportional to their specific surface. The most common clays are *Montmorillonite*, *Kaolinite* and *Illite*.

Name	Type	Specific Surface (m^2g^{-1})	C.E.C (meq/100g)
Kaolinite	1:1	10-30	3-15
Illite	2:1	100-175	25-40
Montmorillonite	2:1	700-840	80-100

Table 1.3: Characteristics of the most common clays

1.5 Durability of soil-mixing material

1.5.1 Chemical attacks

The durability of concrete in sulfate environment depends on several factors, such as the permeability of the concrete, the type of structure, the concentration and type of sulfate, the water table and the mobility of the groundwater. On the other hand, the sulfate attack on concrete is a complex phenomenon, where chemical and physical aspects should be considered. The mechanism of sodium sulfate attack can be divided into ettringite formation, gypsum formation, and salt crystallization [6]. All products occupy a greater space than the original compounds causing expansion and cracking. For gypsum and ettringite formation, the volume increases about 1.2 and 2.5 times, respectively, whereas the crystallization of Na_2SO_4 causes expansion about 4 or 5 times the original volume.

Mode of sulphate attack Deterioration of concrete due to sulfate attack manifests itself mainly in two forms[7]. The first mode of deterioration is akin to eating away of the hydrated cement paste and progressively reducing it to cohesionless granular mass leaving the aggregates exposed. This type of deterioration may lead to reduction in the cross-sectional area of the structural component(i.e., loss in weight of concrete) and decrease in strength.This mode of failure is attributed mainly to the formation of gypsum. The second mode of deterioration,which is normally characterized by expansion and cracking, takes place when the reactive hydrated aluminate phases, present in sufficient quantities,are attacked by sulfate ions, thereby forming tricalcium-sulfo-aluminate hydrate, also called ettringite. This expansive type of reaction is ascribable to the formation of a colloidal form of ettringite in high pH media.

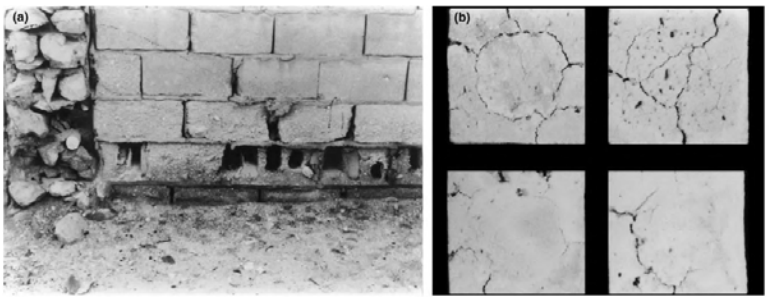

Figure 1.5: Modes of sulfate attacks -Formation of a) Gypsum and b) Ettringite

1.5.2 Carbonation

Carbonation is a process by which carbon dioxide (CO_2) in ambient air penetrates soil-mixing materials through the porous structure and once dissolved in water reacts with cementitious matrix. The reaction occurs with cement hydrates such as calcium hydroxides (Portlandite $Ca(OH)_2$) and calcium–silicate–hydrate (C–S–H) gel in the cement paste matrix to form calcium carbonates ($CaCO_3$). These chemical reactions are expressed as follows:

$$(1) \quad Ca(OH)_2 + CO_2 \rightarrow CaCO_3 + H_2O$$

$$(2) \quad (CaO)x(SiO_2)(H_2O)y + xCO_2 \rightarrow xCaCO_3 + (SiO_2)(H_2O)t + (yt)H_2O$$

Unhydrated cement also reacts with CO_2, as expressed by the following reaction equations:

$$(3) \quad (CaO)_3(SiO_2) + (3x)CO_2 + yH_2O \rightarrow (3x)CaCO_3 + (CaO)x(SiO_2)(H_2O)y$$

$$(4) \quad (CaO)_2(SiO_2) + (2x)CO_2 + yH_2O \rightarrow (2x)CaCO_3 + (CaO)x(SiO_2)(H_2O)y$$

In the field of concrete engineering, carbonation is one of the main causes of the corrosion of steels embedded in reinforced concrete structures, and therefore, it has attracted considerable research attention [9]. Carbonation significantly lowers the alkalinity of concrete via the consumption of $Ca(OH)_2$. This decrease in alkalinity destroys the passive protective oxide film around steel, causing it to start corroding.This is an important factor for some Deep Soil Mixing constructions where steel is inserted in the soil mixing matrix in order to reinforce the resistance to shear stress and bending moments. In general calcium carbonate causes variation in volume and by cracking there is a fall in strength and in permeability. Simultaneously, the generation of carbonates by carbonation changes the pore structure of concrete, often increasing the density of the pore structure and thereby increasing the soil-concrete strength.
Studies on the carbonation of cement-treated soils have mainly aimed to improve cement-based solidification/stabilization of heavy metals by accelerated carbonation techniques [9]. Accelerated carbonation techniques supply carbon sources such as gaseous (CO_2) or sodium carbonate (Na_2CO_3) during soil mixing. These carbon sources can activate the reaction of unhydrated cement, increase the early strength of the mixture and reduce the leaching of heavy metals and alkalinity.

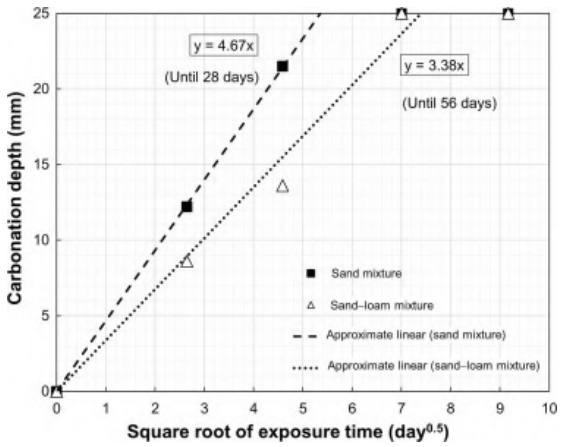

Figure 1.6: Relationships between the carbonation depths and the square root of the exposure time for sand and sand-loam mixtures

1.6 High temperature behavior

The concrete itself has excellent fire resistance properties and seen its large use in construction it is easily subject to fire thereby a complete knowledge of material behavior at high temperatures is necessary. The chemical and physical processes that occur during fire are different in function of the temperature and among the significant effects there is the decay of mechanical properties as the temperature increases. Concrete is a non-homogeneous material consisting of cement paste(cement and water) and aggregates and each component has a completely different response when subjected to high temperatures.

Chemical-physical reactions When the concrete is subject to fire, the increase of the temperature inside the section of the element is gradual and high gradients tend to develop between the external surface and the inside of the section, increasing the damage to which the element is subjected.
In general the material under fire goes through numerous changes in its microstructural,thermal, hydraulic and mechanical behavior. Very common is the loss of strength due to the formation of cracks and decomposition of cement paste and also the cohesion between the cement paste and aggregates is a significant factor. It is therefore necessary to study the different processes that take place in the concrete matrix. The transformations are summarised in the table 1.4.

Most of these reactions cause a significant increase in volume and the difference of expansion between aggregates and cement paste can produce cracks and detachments. Experiments have shown that the expansion of siliceous aggregate is higher than those of calcareous.

Since in this study the cement is mixed with soil it is also important to know how the soil behave when subjected to high temperature. Foldvari [15] studied different types of clays. The Fig.1.7 shows the results of an ATG/ATD of Na-montmorillonite. The diagram of the differential thermal analysis (DTA) of the Montmorillonite has two endothermic peaks between 100 and 200 °C and at 750 °C respectively; the first is due to the alienation of the water originally present in the interlayers while the second derives from the removal of hydroxyls. The Thermogravimetry analysis (TG) shows , in correspondence of the two endothermic peaks of the DTA, two weight losses.

Temperature (°C)	Transformations	Strength
$<$ 95-100	Evaporation of freeH_20	Intact
135	Ettringite decomposition and dehydration $3CaO \cdot Al_2O_3 \cdot 3CaSo \cdot 32H_2O$	Pratically unaltered
135-350	Dehydration of the silicate gel hydrates $nCaO \cdot SiO_2 \cdot mH_2O$	Gradual modest reduction
450-520	Dehydration of calcium hydroxide $Ca(OH)_2 \rightarrow CaO + H_2O$	Progressive reduction
560	α-quartz turns into β-quartz (siliceous aggregates)	Further reduction
700-900	Decomposition of calcium carbonate $CaCO_3 \rightarrow CaCO + CO_2$	Greatly reduced
900-1200	Total dissolution of concrete	Zero

Table 1.4: Chemical and physical transformations in concrete subject to high temperatures

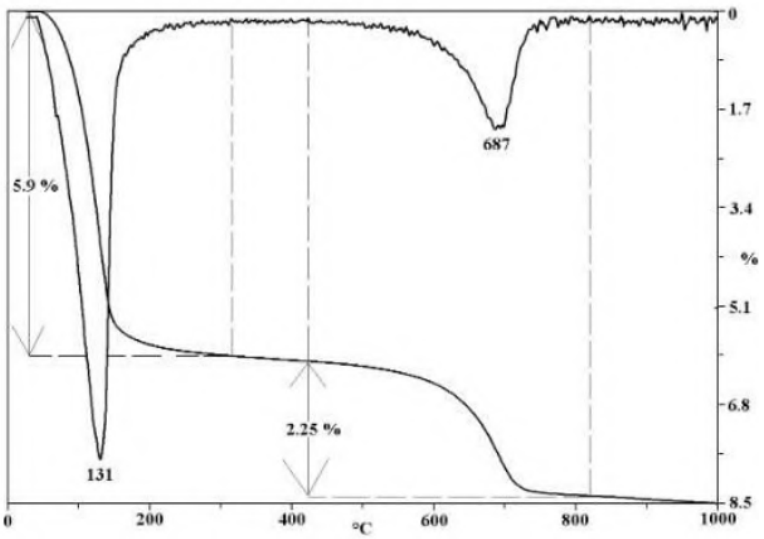

Figure 1.7: Typical TGA/TDA diagrams of primary Na-montmorillonite

Studies have been carried out on soil mix material too. The TGA study results for the original clay and for the lime and fly ash treated clay specimens are shown in Fig. 1.8 [12]. The sudden dip signified as a weight loss for the dehydroxylation of montmorillonite between 450 and 600 °C, appears to be much smaller for untreated clays than that for stabilized clays. The weight loss occurring for the original untreated sample between 450 and 600 °C is due to the breaking of the crystalline structure of Montmorillonite which results in rearrangement of octahedral and tetrahedral structures of alumina and silica[14]. Thus, the stabilization process occurs for the untreated soil as the swelling characteristics of the expansive soil is reduced due to the enhanced breaking of Montmorillonite bonds in the stabilized soils indicated by sharper peak drops in figure 1.8.The sharper peak drops for treated soil clays accounts for the unreacted hydrated calcium carbonate which decomposes to release CO_2 and CaO and hence the increased weight losses. Also, additional losses have been developed at temperatures from 115 to 150 °C for treated stabilized soil samples, thus confirming the formation of CSH or CAH, which was initially absent in the untreated soil samples. The weight loss occurring between 115 to 150 °C, was 0.131 % for only soil, 0.187 % for soil + 20 % fly ash and 0.455 % for soil + 20 % Fly ash + 8.5 % lime, thus indicating the increased presence and decomposition of calcium silicate hydrate (CSH) and calcium aluminate hydrate (CAH) at these temperatures in the treated soil samples.

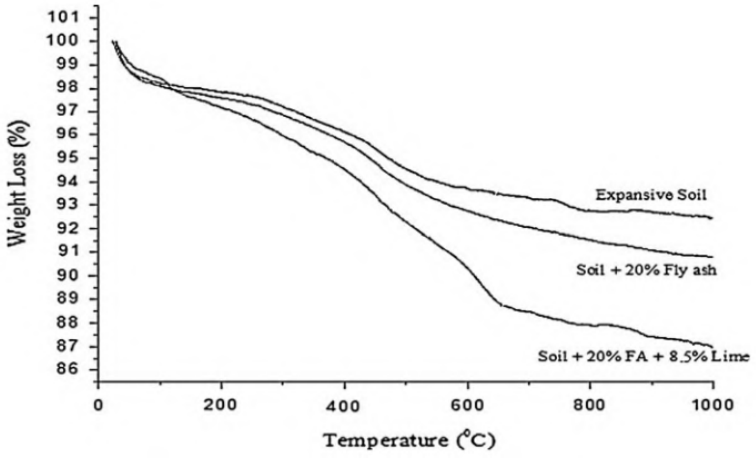

Figure 1.8: TGA results for untreated and stabilized soils

Jean-Claude Morel[13] studied a soil concrete mixture with kaolinite, quartz, goe-thite, hematite, rankinite as well as calcite and portlandite.Regarding the thermal results (Figure 1.9),the endothermic effects at about 80, 350, 520 and 567 °C were linked to dehydration water, loss of crystallization water of dehy-

droxylation of kaolinite and to the transformation of quartz α to β, respectively. The exothermic effect at about 320 °C expressed the combustion of organic matters. The weak thermal effect at 120 °C was due to the dehydroxylation of calcium silicate hydrate (CSH), when the one at 472 °C was attributable to the dehydroxylation of portlandite. The marked endothermicphenomenon at about 750 °C was linked to the transformation of calcite to lime.

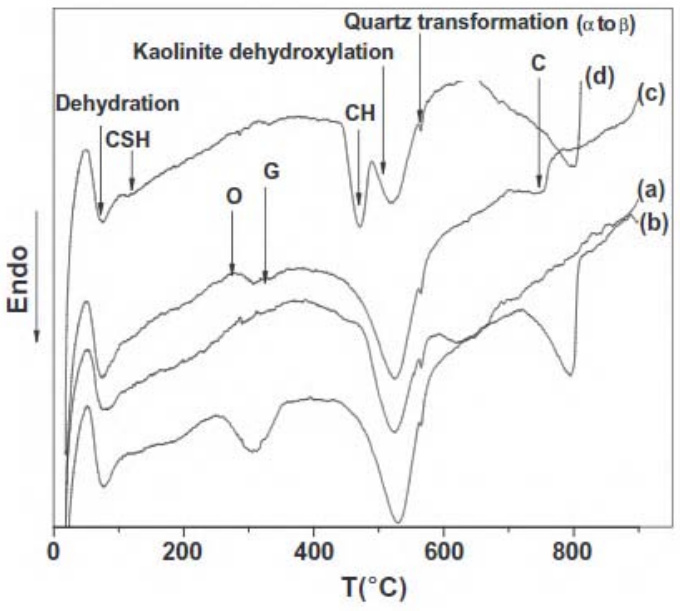

Figure 1.9: DTA curves of the lime mixes samples: (a) raw, (b) 2 wt.% lime, (c) 3 wt.%lime, and (d) 8 wt.% lime

Chapter 2

Experimental Investigation

2.1 Materials

2.1.1 Soil

The soil used in this study comes from a construction site (Esbly). The soil is taken at different depths : 1, 2 and 3 meters. The soil mixed with cement is considered as the aggregates for ordinary concrete. It is important then to define its characteristics in order to understand all chemical and physical processes associated to soil-cement material.

Grain Size Analysis

The distribution of different grain sizes affects the engineering properties of soil. Grain size analysis provides the grain size distribution in order to classify the soil.The grain size analysis is performed to determine the percentage of different grain sizes contained within a soil. The mechanical or sieve analysis is performed to determine the distribution of the coarser, larger-sized particles, and in the same way finer particles, using a water-process method, according to the standard XP P94-041.
The test consists of separating by washing the agglomerated grains of a sample of soil, knowing its mass. Then the grains are fractionated using a series of sieves and the remaining part after drying, cumulated over each sieve, is weighed.
The nominal dimensions of the mesh opening is chosen in function of the nature of the sample and grain levels used for classification. The masses are reported to the initial dry mass of the sample under test. In the standard the minimum diameter imposed is 80μm , however, in order to obtain more information also the sieve of 63μm and 40μm were used. The test procedure consists of the following

steps :

- Soak of 20 kg of soil into water for at least 72 hours
- Mix the oversaturated soil gravimetrically using a tube after removing the excess of water;
- Wet sieving from 630μm to 40μm

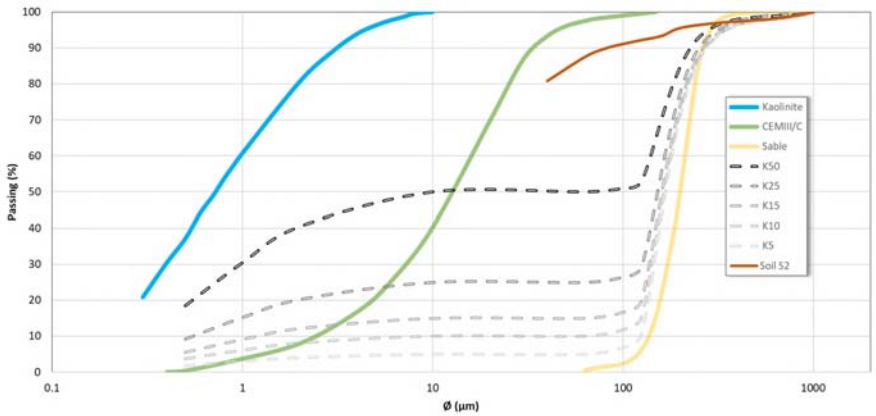

Figure 2.1: Grain size curves

The results show that the soil S_2 is a silty clay, in fact at 40 μm the soil passing is 80 %.

Atterberg Limits

Soils show different states of stability depending on the water content. This property is described as consistency and specifies the state of a remolded and cohesive soil. The states range from solid state to liquid state in the following order:

- Solid limit
- Semi-solid limit
- Plastic limit
- Liquid limit

In the early 1900s, the Swedish chemist Albert Atterberg developed a classification system and method with which these states of consistency could be determined. The method is based on the determination of the water content at

distinct transitions between different states of soil consistency. The liquid and plastic limits are the most commonly used. The values for these limits are dependent on various soil parameters (e.g., particle size, specific surface area of the particles that are able to attract water molecules). These limits are used to derive indices (e.g., index of plasticity and index of consistency) and are often used for the mechanical characterization of soils.

Liquid Limit The Liquid Limit, also known as the upper plastic limit, is the water content at which the soil changes from the liquid state to a plastic state. It is the minimum moisture content at which a soil flows upon application of very small shear force. The precise definition of the liquid limit is based on standard test procedures. Liquid Limit can be determined using the Casagrande cup method (Figure 2.2).

Figure 2.2: Casagrande cup

According to this method, the soil paste is placed into the Casagrande cup and a groove is made at the center of it. The limit is defined as the moisture content, in percent, required to close a distance of 13 mm along the bottom of a groove after 25 blows in a liquid limit device. Hence, at least three tests for the same soil are conducted at varying moisture contents, with the number of blows (N), varying between 15 and 35. If the value of N is lower than 15 or higher than 35 the test must be repeated.

The test procedure to find the Liquid Limit consists of the following steps :

- Place a soil paste in the cup
- Cut a groove at the center of the soil paste with the standard grooving tool

- Lift the cup and drop it from a height of 10mm, using the crank-operated cam.
- Measure the water content required to close a distance of 13 mm along the bottom of the groove and note down the number of blows.

The data are plotted in a graph and by drawing the best-fit straight line through the plotted points the value of the liquid limit is obtained. The moisture content corresponding to N=25, determined from the curve, is the liquid limit of the soil.

Plastic limit The Plastic Limit, also known as the lower plastic limit, is the water content at which a soil changes from the plastic state to a semisolid state. The Plastic limit test is performed by repeated rolling of an ellipsoidal-sized soil mass by hand on a non-porous surface. Casagrande defined the plastic limit as the water content at which a thread of soil just crumbles when it is carefully rolled out to a diameter of 3 mm. If the thread crumbles at diameter smaller than 3 mm, the soil is too wet. If the thread crumbles at a diameter greater than 3 mm, the soil is drier than the plastic limit. The sample can then be remolded and the test repeated. Once the appropriate size rolls are made, their moisture content is assessed using the procedure described previously. At least three measures for the estimation of the plastic limit in order to obtain a reliable value of the plastic limit.

Atterberg limits are determined in accordance with standard NF P94-051(1993-03-01), while the water content is determined in accordance with the standard NF P94-051. The value of liquid limit is used to calculate the water content of the soil-cement mixtures.

2.1.2 Cement

The type of cement used is CEM III/C 32.5 N, CE PM-ES NF (NF EN 197-1 2012), in accordance with the european classification.

This type of cement contains more than 85 % of blast furnace slag, responsible of the slow development of resistance but whose latent nature is favourable as regards workability. Due to the consumption of the Portlandite during hydration, slags are more sensitive to carbonation and therefore less suitable in the presence of reinforcement in concrete. The CEM III/C remains one of the most used

cement in France in the field of foundations, since its composition confers to the concrete an excellent resistance towards chemical attacks and reduces the permeability. This cement is further considered to be eco-efficient in view of its low CO_2 emission. The manifacture of a CEM III/C produces about 10 time less CO_2 than a CEM I. Its low environmental impact is possible through the development of by-products of steel industry wich makes it one of the cement with lower rate of clinker.

Type of BFSC	Clinker (mass %)	Minor additional constituents (mass %)
CEM III/A	35-64	36-65
CEM III/B	20-34	66-80
CEM III/C	5-19	81-95

Table 2.1: Composition of blastfurnace cements (BFSC)

The composition of cement CEM III/C is shown in the following table :

CEM III/C		
Elemental composition	(%)	Constituents
SiO_2	32.8	Clinker (K) 15 %
Al_2O_3	10.2	Slag (S) 85 %
Fe_2O_3	0.7	Ashes (V)
CaO	46	Limestone (L or LL)
MgO	5.5	Silica fume (D)
SO_3	2.9	Gypse 5.5 %

Table 2.2: Composition of cement CEM III/C (Calcia)

2.2 Mixing, conservation, testing procedures

The soil-concrete material was manufactured in the laboratory. The aim is to obtain a homogeneous material in order to facilitate the mixing.
First the soil is submerged in the water for 72 hours so that it is completely saturated, then after sedimentation the clear water is recovered gravimetrically using a tube and during this operation the fine part of the soil must not be removed. The rest of the moist soil is subsequently mixed for 5 minutes. Then the water content is determined and as explained in the next section the amount of water

addition is calculated in order to obtain a 50% of water content for the total mixture. When the mixture is ready the soil is put in a mixer Controlab (Figure 2.3) and mixed for 10 minutes with a speed of 63 revolutions per minute.The material was then mixed for 10 minutes because beyond the mixing has no more effect on the strenght of hardened concrete.

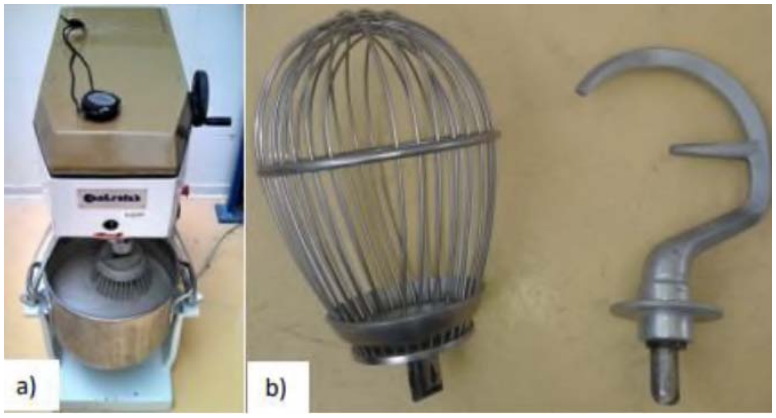

Figure 2.3: a) Mixer Controlab b) Tools

Water content of the mixes was chosen in order to achieve a self-compacting material, meaning that it should be fluid enough to flow under its own weight. Thus, the water content must be at least equal to the liquid limit of the mix [4]. This water content is calculated as follow : water originally contained in the soil plus any water added during mixing over the dry mass of the soil. The mix was then poured into cylindrical moulds of 60 mm diameter and 120 mm of heigth, and, to avoid air bubbles in the specimens, were tapped (15 blows) after filling the moulds in three successive layers.
The specimens of soil-concrete material are then demoulded after 7 days of curing time. A time long enough to allow the material to reach an adequate strenght, in order to not damage the specimens by removing them from the moulds. The samples are subsequently wrapped into wet rags to avoid premature drying. The method of cure is the one with water that keeps the specimens satured.

2.3 Mix design

The concrete mix design phase consist in find the optimal mixture of soil, cement and water. The aim is to create a concrete with pursued characteristics. The soil was taken at different depths : soil at 1 meter depth (S_1) , soil at 2 meters depth (S_2) and soil at 3 meters depth (S_3). In this study the soil (S_2) was mainly used

investigating three different cement dosages of 200, 250, 300 kg/m^3per m^3 of soil mixed material. The same total water content of 50 % was kept constant for all mixtures. The table below shows the material characteristics.

ρ_{cement} (kg/m^3)	ρ_{soil} (kg/m^3)	ρ_{water} (kg/m^3)	$\rho_{wetsoil}$ (kg/m^3)	$water_{soil}$ (%)
2900	2650	1000	1679-1880	33-54

Table 2.3: Material characteristics

The method used to determine the formulations starts first of all fixing the value of the cement dosage. Then the ratio W/C is chosen intuitively, and the quantity of soil is derived in order to obtain $1m^3$ of fresh concrete. The composition of 1 m^3 contains :

- M_{sm} moistened soil mass with its water content w_{sol}
- M_c cement mass CEM III/C 32.5 N
- M_{aw} mass of water added

The air contained in the mixture is neglected. These masses are calculated in order to keep the water content of soil-mix concrete at 50 %.

Once the cement dosage is chosen (M_c), the value of dry soil (M_s) and water mass (M_w) for 1 m^3 of cement-soil mixture can be obtained.

$$\begin{aligned} M_c + M_s + M_w &= M_{mix} \\ V_c + V_s + V_w &= 1m^3 \\ \frac{M_c}{\rho_c} + \frac{M_s}{\rho_s} + \frac{M_w}{\rho_w} &= 1m^3 \end{aligned} \tag{2.1}$$

The water content is

$$w = \frac{M_w}{(M_c + M_s)} \tag{2.2}$$

The results are shown in the following table :

Cement (kg/m^3)	Dry soil (kg)	Wet soil (kg)	Added water (kg)	Density (kg/m^3)	Total W/C
100	1043	1156	459.7	1715	5.72
150	995	1102	466	1718	3.82
200	947	1049	472	1721	2.87
250	899	995.6	478	1724	2.30
300	851	942	484	1726	1.92

Table 2.4: Mix design parameters for one m^3 of soil-cement mixture

2.4 Physical Properties

2.4.1 Porosity

The porosity accessible to water is also measured. The tests are carried out using cylindrical specimens of 60 mm diameter and of 120 mm high. First of all the specimens are dried in an oven at 60 degrees until they reach a constant mass and this procedure is repeated for different time of maturation. The drying temperature is intentionally lower than that recommended by the standard in order to limit the thermally-induced stresses, that lead to cracking. Once dry, they are weighed and then placed under vacuum in a desiccator for two hours. In this way the complete saturation in the water is facilitated and makes it possible to fill most of the pores bringing up water thanks to capillarity. After three days submerged in water the samples an hydrostatic weight and a weight in a saturated state are measured to calculate the value of the porosity according to the standard NF P 18-459.

$$\eta = \frac{M_{air} - M_{sec}}{M_{air} - M_{eau}} \tag{2.3}$$

where M_{air} the mass of the specimen saturated and dried on its surface (g), M_{sec} the mass of the dry specimen (g) and M_{water} the mass obtained using the hydrostatic weighing method (g).

2.4.2 Density

The fresh-state density is determined experimentally : after mixing a two liters container is filled with soil concrete.

In the case of wet density (ρ_h) the result is determined by weighing with a balance ($\pm$ 0.02 g) and the dimensional measurements with a caliper ($\pm$ 0.1 mm). The size of the specimen is measured once the sample is sanded and just before the compression tests.

$$\rho_h = (\frac{M_{hum}}{V_{hum}}) \tag{2.4}$$

where M_{hum} the mass of the sample when moist (kg) and V_{hum} the apparent volume of the sample measured with the caliper (m^3).

2.4.3 Dimensional stability

Shrinkage and swelling tests were conducted according to NF P 15-433 for hydraulic mortars. These test comprise measuring, as a function of time, the variation of the length of the specimens in the air for the shrinkage test and in the water for swelling test, following their removal from the mould. The size of the moulds are 4x4x16 cm, pierced along the longitudinal axis at the extremities to secure metal terminal pads,needed for the measures, during the curing phase. The specimens are removed from the mould after three days of maturation. The measure is then carried out using a steel frame provided with a comparator (Figure 2.4) : the specimens are placed between the two sensors (or feelers) of the device,equipped with bearings, the metal pins which are inserted in order to assure a proper positioning. The reset at the zero of the device is performed using a metal rod 160 mm long. At the end this device can measure the dimensional variations upon exposure to air (shrinkage) or to water (swelling) of samples.

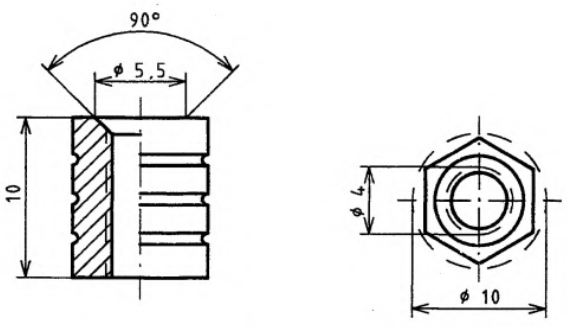

Figure 2.4: Measure of dimensional variation

In this case only the test of exposure to water is conducted. The specimens are kept entirely submerged without contact with one another at 20 degrees. The specimens are taken out of the water 15 minutes before measuring. The test piece is disposed vertically and and undergoes a complete rotation on its axis before

the measurement. The change in relative length is calculated as the difference between the original measurement at mould release and the final measurement. This variation, specified in micrometers per meters, is defined by the following formula :

$$(\frac{dL}{L}) \cdot 1000 \tag{2.5}$$

where dL is the variation of the length of the specimen in micrometers and L is the basic length of 160 mm.

2.5 Permeability

The test equipment of triaxial cell provides, under a known pressure difference, a water flow through a sample. In that way it is possible to measure the flow rate meanwhile the sample is subject to a known effective stress.

Figure 2.5: Device for the measure of the hydraulic conductivity

Table 2.5 lists each primary component of a GDS triaxial system, along with its main function.

Procedure The test specimen itself must firstly be prepared before placing into the cell. A membrane suction stretcher can be used to place the rubber membrane around the soil once in position on the pedestal. Then the sample is placed in the confinement cell between two porous stones in order to uniform equally the water pressure at the level of the upper and lower surfaces of the sample and thereby avoid locating flows of water. Filter papers are placed at each end of the sample in order to prevent the migration of particles into the devices. The waterproofness is insured between the sample and the water in the confinement cell by a latex membrane and two ring type joints at each end.

Component	**Main function**
Triaxal cell	House the specimen and cell fluid
Pedestal and top-cap	Provide specimen seating and drainage ports
Rubber menbrane, O-rings and porous discs	Seal the specimen from the cell fluid, allowing control over the effective stress and drainage
Cell pressure/volume controller	Apply confining stress to the specimen ($\sigma_c - \sigma_3$) by pressuring the cell fluid
Back pressure/volume controller	Apply back/pore pressure u to the specimen and measure volume change ΔV
Velocity controlled load frame	Shear the specimen through axial movement of a loading platen at a constant rate
Internal submersible load cell	Measure the change in axial load F applied to the specimen during shear
Pore water pressure transducer	Measure the change in pore water pressure u within the specimen
Axial displacement transducer	Measure the change in height (and hence axial strain) of the specimen

Table 2.5: Primary components of a GDS triaxial automated system

Following placement of the specimen, the cell and other system components are assembled. During this stage the cell is filled with fluid, pressure / volume controllers connected, and transducer readings set as required. The test starts with the measure of the Skempton (β) coefficient, which corresponds to the increase of the pore pressure at the level of the lower valve (the upper one is closed) divided by the gradient of the confinement pressure applied on the sample. The saturation process is designed to ensure all voids within the test specimen are filled with water, and that the pore pressure transducer and drainage lines are properly de-aired. The measuring cylinder of soil concrete is at first saturated under vacuum. To assist the specimen in reaching full saturation, the following steps may be taken:

- Use of de-aired water to fill specimen voids.
- Increase of back pressure to force air into solution.

To check the degree of specimen saturation is sufficiently high before moving to the consolidation stage, a short test is performed to determine Skempton's B-value (Figure 2.7)

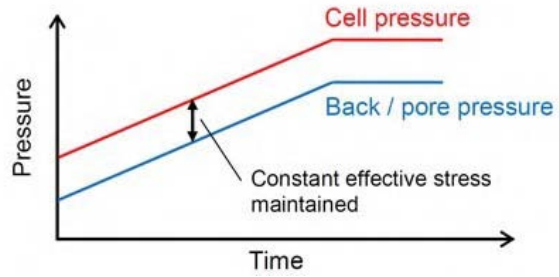

Figure 2.6: Specimen saturation by increasing back pressure

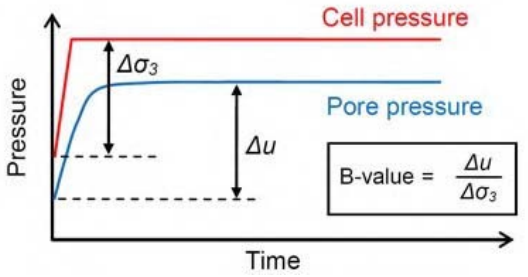

Figure 2.7: β-check to confirm specimen saturation.

The coefficient is measured until is stable in order to assure that the sample is completely saturated before starting the permeability test. When β is equal to one, that's mean that the material is considered as saturated and incompressible, but more the coefficient is lower and less than 1, also the material is more compressible.Note however that B is soil-dependent, so whilst a normallyconsolidated soft clay will produce B $\simeq$ 1.00 at full saturation, a very dense sand or stiff clay may only show B $\simeq$ 0.91, even if full saturation has been reached. The coefficient is determined by a pressure increment of 100 kPa (up to 500 kPa).Different tests are taken in order to verify that the permeability doesn't change in response to hydraulic gradient changes, instead depending on the effective pressure. Then it is possible to calculate the permeability from the following equation:

$$k(m/s) = R_T \cdot \frac{Q \cdot \mu \cdot L}{\Delta P \cdot A \cdot \rho} \cdot 10^7 \tag{2.6}$$

where

- R_T - Correction factor (temperature)
- Q - Water flow through the sample (kg/s)
- ρ - Density of water (kg/m^3)
- μ- Dynamic viscosity of water (Pa $\cdot$ s)

- L - Height of the sample (m)
- A - Section of the sample (m^2)
- ΔP- Pressure difference between the two ends of the sample (Pa)

2.6 Mechanical properties

Compressive strength and E_{stat} In this study the mechanical properties are determined using both hydraulic press SCHENK (3000 KN) and the load frame of the triaxal device, used to determine the value of the permeability.These presses were used to determine the compressive strength of cylindrical specimens. The specimen is placed on the lower face of the press and the upper part applies the compressive charge.

Figure 2.8: Schenck press

Figure 2.9: GSS press

According to the standard NF P 18-406 the specimens tested to unconfined compression have an elancement of two : their diameter is of 60 mm and the height of 120 mm after surfacing. In fact the specimens are actually surfaced before the loading phase, in order to provide a uniform distribution of the load. The method used to surface the extremities of the specimen is the sulfur-based surfacing.So the surfaces were covered by a sulfur layer (Figure 2.10). The sulfur is liquefied at the temperature of almost 150-180 °C, then poured on a specific instrument (Figure 2.10b), and the specimens put vertically on the liquid sulfur.

After some minutes, the sulfur solidifies and the same operation is repeated for the other face, obtaining the final results shows in Figure 2.10a.

Figure 2.10: Equipment employed in surfacing with sulfur

The loading is performed under controlled stress at a speed of 0.6 mm/min. The choice of a low loading speed is due to give the time to cracks to spread during the test. The compression strength (MPa) is calculated from the following equation:

$$f_c = \frac{F_c}{A} \tag{2.7}$$

with F_c is the ultimate resistance in compression (MN) and A the section of the specimen.
Once the test has been carried out and the data collected, the value of the modulus can be calculated as follow :

$$E = \frac{\sigma}{\epsilon} \tag{2.8}$$

where σ is the stress (MPa) and $\epsilon = \Delta l/l$ the strain. The module of elasticity is calculated from the displacement of the trays of the press.The method of determination is shown in the figure 2.11 and consists in taking the point of maximum (fc_{max}) and then the trend line of the stress-strain curve is traced from a range of values between $0.1fc_{max}$ and $0.5fc_{max}$ and the value of E is the slope of the straight line.This global measurement method is less accurate than the local measurement method which involves the use of the strain gauges in order to de-

termine the static modulus of elasticity. The method used usually underestimates the value of the Young's modulus.

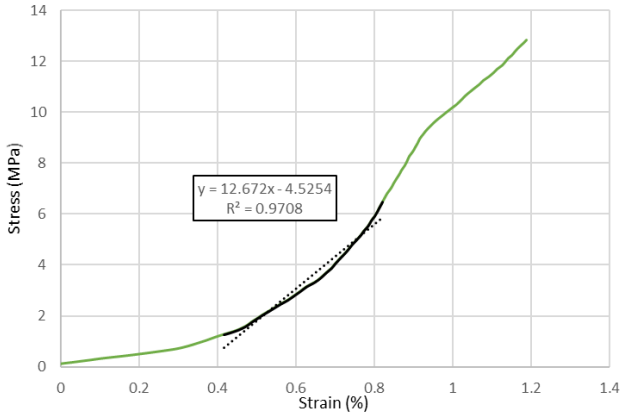

Figure 2.11: Determination of E

E dynamic Regarding instead the dynamic modulus of elasticity the equipment used is the *Pundit7* (Figure 2.12), a device able to measure the compression wave speeds (V_p). During the test an ultrasonic signal is transmitted as a pulse and then the propagation through the sample is analysed. The ultrasonic wave travel time between two piezoeletric transducer with a frequency of 54 kHz, a transmitter and a receiver, placed in contact with the sample facing each other. The ratio between the distance traversed by the wave P and the time of travel gives the value of the propagation speed.

Figure 2.12: PUNDIT 7

The test are performed on cylindrical specimens (d=60 mm and h=120mm) in the wet state in function of the curing time and before each compression test. A small quantity of vaseline is applied on the piezoelectric transducer before the

test in order to improve the contact with the specimen and therefore the transmission of the waves.The value of the dynamic modulus of elasticity is calculated by the following formula:

$$E_0 = \rho \cdot V_p^2 \cdot \frac{(1+\upsilon)(1-2\upsilon)}{(1-\upsilon)} \tag{2.9}$$

where ρ is the density (kg/m^3), V_p the wave speed (m/s) and υ the Poisson coefficient (-). Reported values of Poisson's ratio for deep-mixed material ranges from 0.25 to 0.50.

2.7 Thermoanalytical methods

Thermal analysis is a group of analytical techniques in which physical properties or chemical reactions of a substance are measured as a function of temperature.

Thermogravimetry The TG is a technique in which the mass of a substance is measured as a function of temperature while the substance is subjected to a controlled temperature programme. In this study TGA is used to investigate in order to calculate the water content related to the dehydration of C-S-H, Ettringite and Portlandite. The test consists first of filling a crucible with about 100 mg of a sample previously crushed. The crucible is calibrated and handled with a plier. The sample is heated to 10 °C per minute until 1100 °C in an inert atmosphere.

Differential thermal analysis The DT analysis is a technique in which the temperature difference between a substance and a reference material is measured as a function of temperature whilst the substance and reference material are subjected to the same controlled temperature program.The technique requires the use of a reference material, which is a known substance, usually inactive thermally (inert material) over the temperature range interest.An important feature of the reference material is that the thermal characteristics (specific heat, conductivity etc.) and the particle size should be very similar to that of the sample. The record of the ATD curves allows, by identifying endothermic and exothermic peaks, to trace back to products derived from the hydration of cement and to trace back to phase changes. TGA and TDA test are conducted at the same time using the NETZSCH device (Figure 2.13)

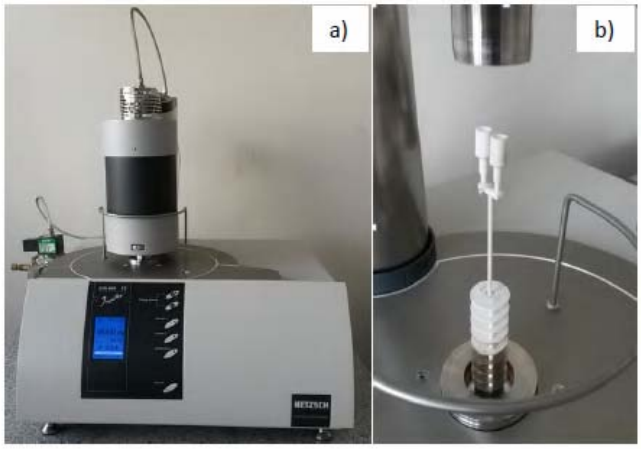

Figure 2.13: a) Device NETZSCH b) Crucibles

2.8 High Temperature

The tests are performed in an electric and programmable oven with a maximum allowable temperature of 1000 °C (Figure 2.14b). This oven is equipped with heater resistors as its side walls and has a specific ventilation in order to uniform the temperature inside the oven during the test. In total, 15 K-type thermocouples were used. These thermocouples were placed on the surface and some in the center of the samples in order to control the heating homogeneity on the specimens. Some of them were also placed to monitor the oven: the regulatory thermocouple and the safety thermocouple. An automatic acquisition system led by a computer (Figure 2.14.a) can record constantly these temperatures.

(a) **(b)**

Figure 2.14: a) Acquisition system b) Oven

The specimens were submitted to heating/cooling cycles. For each cycle there is a heating phase with a rise in temperature of 0.5 °C/min , followed by a two-

hours step during which there is no increase nor decrease of the temperature and a cooling phase at 0.5 °C/min. In this study the specimens (soil S_2) are heated following four different fixed temperature ranges at 200,300,600,850 °C (Figure 2.15).

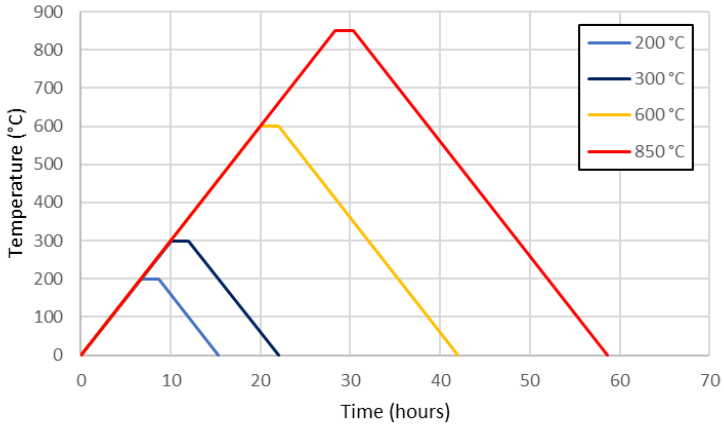

Figure 2.15: Heating and cooling cycles

Chapter 3

Experimental Results

In this chapter the experimental results are presented. They are subdivided in four parts:

- I. Tests to characterise the soil before adding the cementitious binder. The untreated soil investigated has been taken at a depth of one, two and three meters in order to have three different characterisations of the soil and that is because the properties of the soil change with the depth and the results can be compared.
- II. The soil-concrete material characteristics (compressive strength, dynamic and static modulus of elasticity) are evaluated at room temperature (20 °C) and in function of the time.
- III. Study of durability (carbonation and sulphate attacks)
- IV. The characteristics at point II. are evaluated after heating until 200,300,600 and 850 °C

3.1 Soil characterisation

3.1.1 Consistency Limits (Atterberg Limits)

S1 The following graph and table show the results of the tests for the soil taken at a depth of one meter.

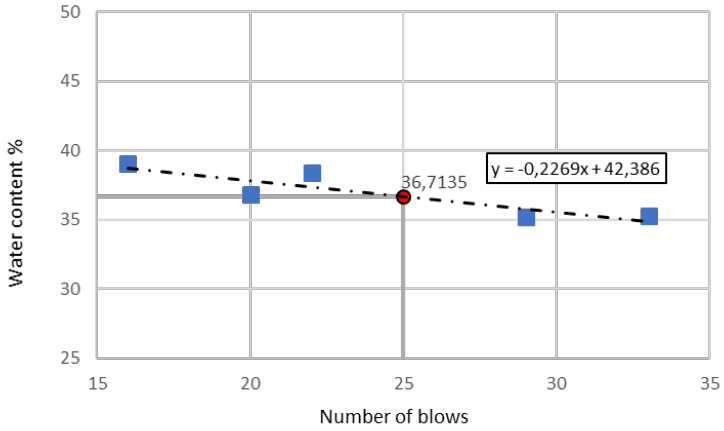

Figure 3.1: Liquid Limit - Soil 1

N	Number of blows	Moist Mass(g)	Dry Mass (g)	Water Mass (g)	Water content (%)
1	22	9.9	7.4	2.5	38.36
2	33	8	6.2	1.8	35.26
3	16	7.5	5.7	1.8	39
4	20	8.6	6.6	2	36.82
5	29	7.7	6	1.7	35.2

Table 3.1: Determination of Liquid Limit - Soil 1 with a mass container for 1.1 g

N	Moist Mass (g)	Dry Mass (g)	Water Mass (g)	Water content (%)
1	5.1	4.5	0.6	17.64
2	4.7	4.2	0.5	16
3	4.7	4.1	0.6	20

Table 3.2: Determination of Plastic Limit - Soil 1 with a mass container fo 1.1 g

The value of the plastic limit is obtained calculating the average of the values of the water content. For the soil S1 the Plastic Limit is 17.9 %

S2 The following graph and table show the results of the tests for the soil taken at a depth of two meters.

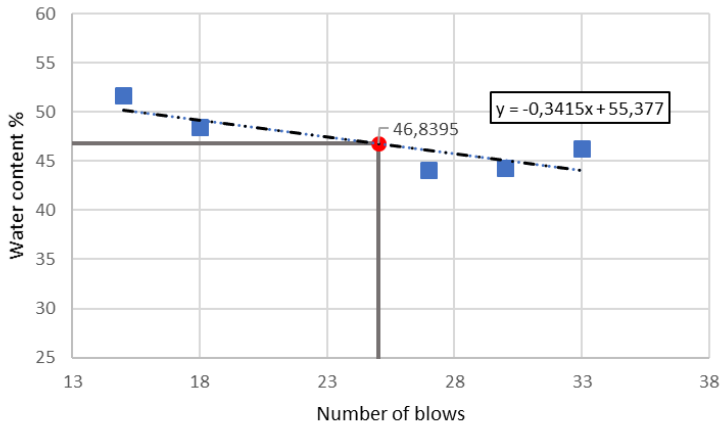

Figure 3.2: Liquid Limit - Soil 2

N	Number of blows	Moist Mass (g)	Dry Mass (g)	Water Mass (g)	Water content (%)
1	27	11.6	8.8	2.8	44.136
2	15	12.4	9	3.4	51.68
3	18	11.3	8.4	2.9	48.5
4	30	12.3	9.3	3	44.3
5	33	11.3	8.5	2.8	46.26

Table 3.3: Determination of Liquid Limit - Soil 2 with a mass container of 2.5 g

N	Moist Mass (g)	Dry Mass (g)	Water Mass (g)	Water content (%)
1	6.5	5.7	0.8	17.39
2	5.4	4.7	0.7	19.4
3	4.7	4.1	0.5	16

Table 3.4: Determination of Plastic Limit - Soil 2 with a mass container fo 1.1 g

The value of the plastic limit is obtained calculating the average of the values of the water content. For the soil S2 the Plastic Limit is 18 %.

S3 The following graph and table show the results of the tests for the soil taken at a depth of three meters.

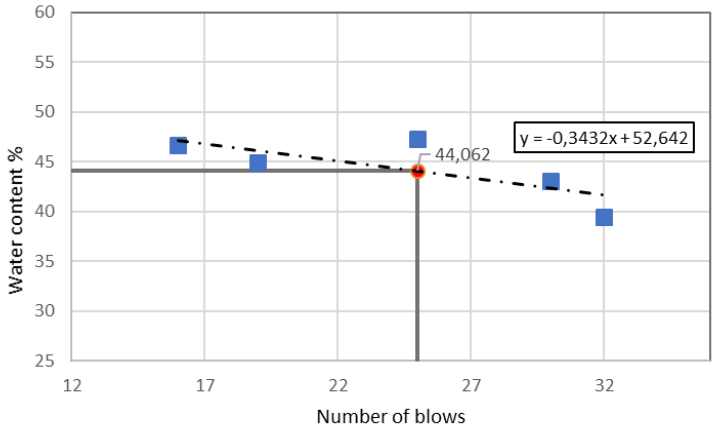

Figure 3.3: Liquid Limit - Soil 3

N	Number of blows	Moist Mass	Dry Mass	Water Mass (g)	Water content (%)
1	32	7.2	5.5	1.7	39.43
2	19	7.2	5.3	1.9	44.9
3	30	5.7	4.3	1.4	43.07
4	25	7	5.1	1.9	47.3
5	16	7.7	5.8	1.86	46.63

Table 3.5: Determination of Liquid Limit - Soil 3 with a mass container of 1.1 g

N	Moist Mass (g)	Dry Mass (g)	Water Mass (g)	Water content (%)
1	3.9	3.5	0.4	16.6
2	3.3	3	0.3	15.78
3	3.3	3	0.3	15.78

Table 3.6: Determination of Plastic Limit - Soil 3 with a mass container fo 1.1 g

The value of the plastic limit is obtained calculating the average of the values of the water content. For the soil S3 the plastic limit is 16 %.

Once the value of the liquid and plastic limit are available the plasticity index can be calculated as the difference between the two limits

$$I_P = w_L - w_P = 36.71 - 17.92 = 18.79 \quad (S_1)$$
$$I_P = w_L - w_P = 46.84 - 18.24 = 28.6 \quad (S_2)$$
$$I_P = w_L - w_P = 44.06 - 16.08 = 27.98 \quad (S_3)$$

The GTR (Guide des Terrassements Routiers) Guide offers a geotechnical classification for soils. The soil can be classified as type A (fine soil) and especially A_2 for soil S_1 and A_3 for soil S_2 and S_3, based on the value of plasticity index and on the results derived from the grain size analysis.

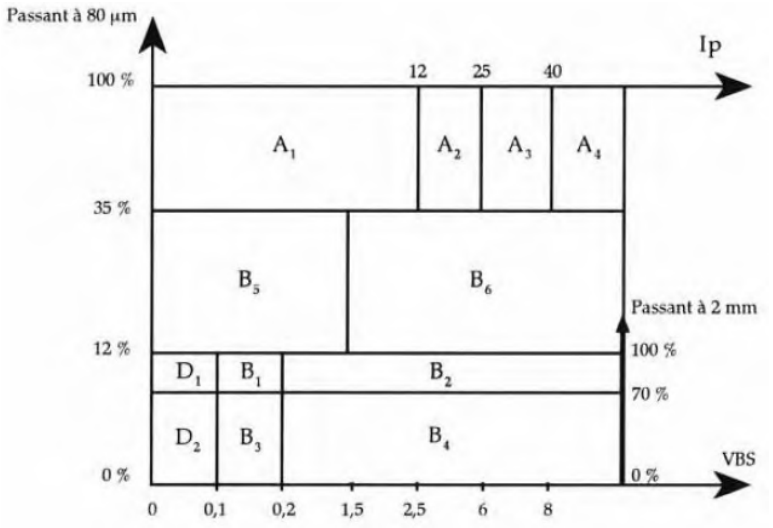

Figure 3.4: GTR Classification

Another system of soil classification is the classification system of *Casagrande* (1948) in Figure 3.5 who identifies six zones and therefore six soil classes in function of the liquid limit and plasticity index. In this case for the soil studied , for all depths, we have a inorganic clay with medium plasticity.

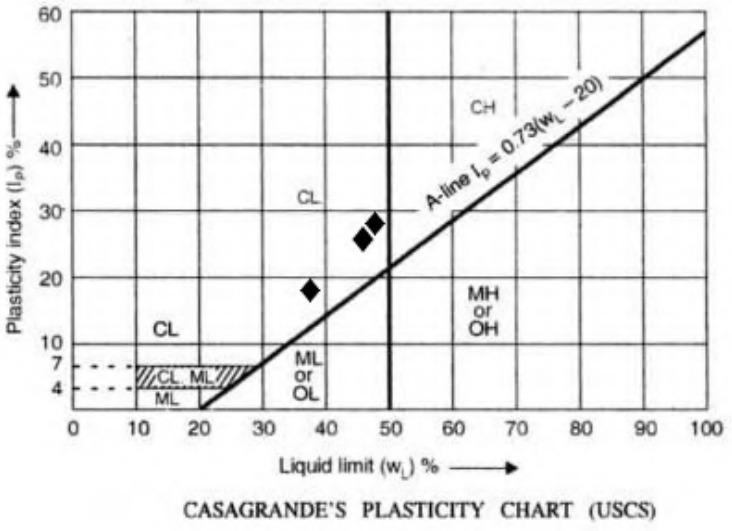

Figure 3.5: Casagrande plasticity chart

3.2 Physical Properties

3.2.1 Hydraulic conductivity

The permeability of soil-concrete mixtures has been calculated in order to investigate one of the physical properties of the material.
The soil S_1 and S_3 were investigated with cement dosages of 100,150,200 kg/m^3. The value of k range from $1.4 \cdot 10^{-11}$ to $9.4 \cdot 10^{-10}$. The results in the table show that the permeability decreases with the cement content. Mixtures with S_3 soil are more permeable than mixtures with S_1 soils and this is related to porosity values.

Specimen	Porosity (%)	Hydraulic conductivity
S_1C_{100}	51	3.00 E-10
S_1C_{150}	50	1.98 E-11
S_1C_{200}	48	1.4 E-11
S_3C_{100}	54	9.38 E-10
S_3C_{150}	54	9.56 E-11
S_3C_{200}	53	1.5 E-11

Table 3.7: Values of hydraulic conductivity

3.3 Mechanical Properties

The compressive strength, static and dynamic modulus of elasticity were determined for different soil-concrete mixtures (soil S_2) . In this section the results of the influence of mixture parameters are investigated and analysed.

3.3.1 Compressive strength

Compressive strength versus time

The values of compressive strength were determined after 7,28,56,90 and 180 days of curing time and each point comes from an average of three specimens tested.

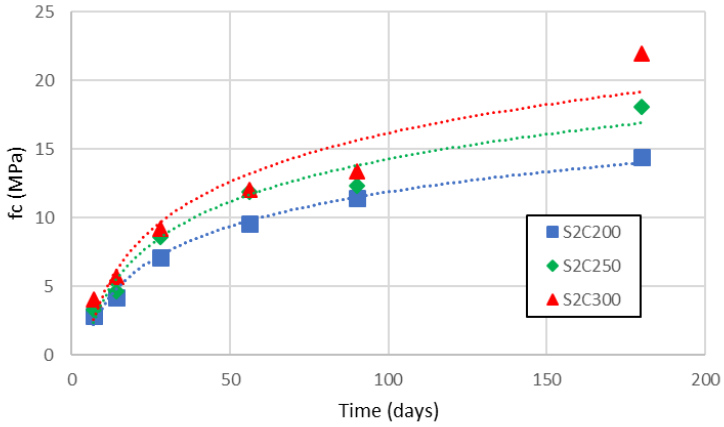

Figure 3.6: Evolution of compressive strength as a function of time

The prolonged increase in strength is largely explained by the type of cement used in this study (CEM III/C); the increase of compressive strength is low because of his high content of blast furnace slags. The strength ranges from 14 to 22 MPa after 180 days of curing time. At this time the value of strength has not reached a constant value and that's mean that there is not yet a stabilisation after 180 days, especially for high cement dosages (300 kg/m^3). The first significant value of strength is achieved after 28 days of curing time. The ratio between the compression strength at 28 and 180 days is in the range of 1.9 for $C_{200}$to 2.4 for C_{300}.

Influence of cement dosage

The increase of the cement content has an impact on porosity and micro-structure of soil-concrete material. These variations reflect at the macro level significant variations in strength and rigidity. In the graph below each point represents the

compressive strength obtained by a cement content of 300 kg/m^3 depending on the values obtained for C_{200} for different curing time (7, 14, 28, 56, 90 and 180 days). It is clearly , thanks to this representation (Figure 3.7), that the gain in strength is related to the increase of the cement content. The trend line shows that the strength is multiplied by 1.42 when the cement dosage goes from 200 to 300 kg/m^3.

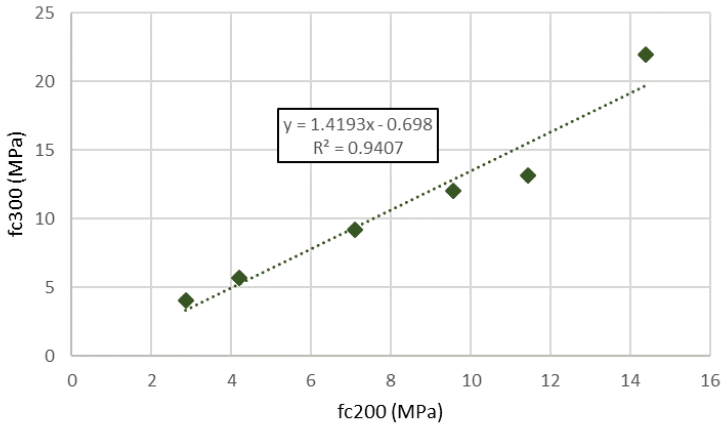

Figure 3.7: Influence of cement content on compressive strength

The following figure shows the 28 days strength in function of the cement content:

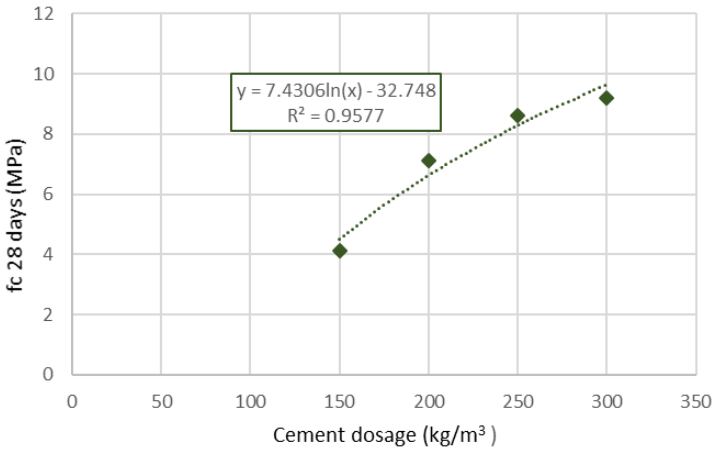

Figure 3.8: Influence of cement dosage on compressive strength after 28 days of curing time

The results show that the compressive strength grows with a logarithmic function with cement dosage:

	f_c200/f_c150	f_c250/f_c200	f_c300/f_c250
S_2	1.72	1.21	1.07

Table 3.8: Influence of cement dosage on compressive strength

$$fc_{28d} = 7.43\ln(x) - 32.7 \qquad R^2 = 0.96 \tag{3.1}$$

The influence of cement dosage is higher for low dosages and on the other hand stronger the dosage, less the increase of cement dosage will be affect the value of compressive strength. The intersection with the x-axis in the Figure 3.8 also highlights that for a cement dosage over 80 kg/m^3 the cement acts as a binder and that there is the change from a soil type behaviour to a soil-concrete mix behaviour.

3.3.2 Static and dynamic elastic properties

Stress-strain curve

The Figure 3.9 shows the three stress-strain curves for each cement dosage obtained during the compression tests. The deformability of the material increases when the dosage cement is lower and this means that the behavior for C_{200} is rather nonlinear associated with a low level of stress. However for the C_{300} specimens the curves indicate further a more linear behavior, while the C_{250} specimens present an intermediate behavior. So for the mixtures with a lower cement dosage the loss of linearity concerns lower loading levels and the susceptibility to damage is higher.

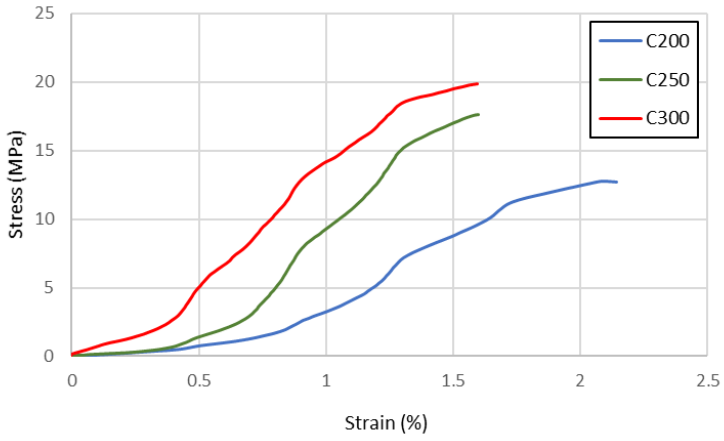

Figure 3.9: Stress-strain curves

E dynamic modulus

The dynamic elastic properties of the material are determined from the P-waves speed, density and Poisson's ratio measurements.
The Figures 3.10 and 3.11 show the value of V_P (waves speed) and E_{dyn} over time. The waves speeds vary between 1885 and 2630 m/s while the dynamic modulus between 4.53 and 8.67 GPa. The values increase with the cement content.

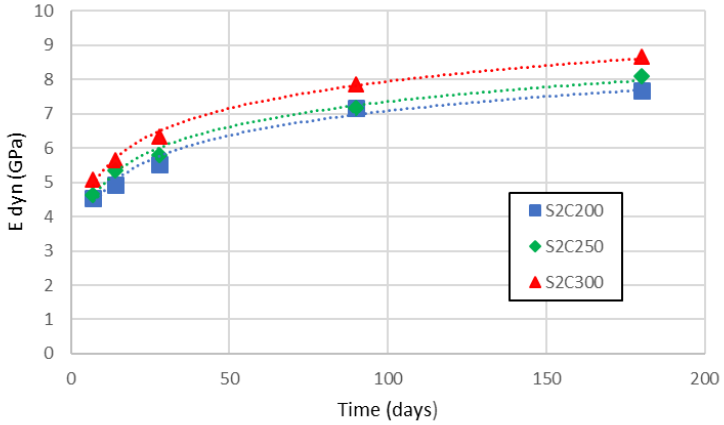

Figure 3.10: Evolution of E_{dyn} as a function of time

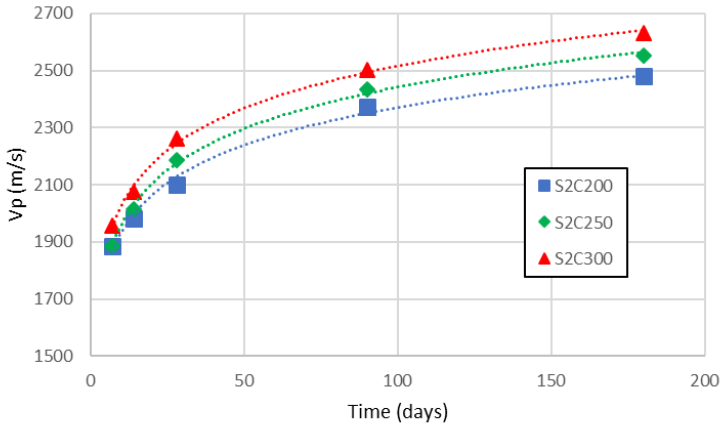

Figure 3.11: Evolution of V_P as a function of time

The Figure 3.12 shows the relation between V_P for C_{200} for C_{300} and each point represents the value of V_P obtained for soil-concrete with 300 kg/m^3 of cement in function of those with a cement dosage of 200 kg/m^3, for a specific curing time and clay content.So non-destructive measurements were performed to study the influence of cement dosage on V_P (waves speeds) between 7 and 180 days of curing time.

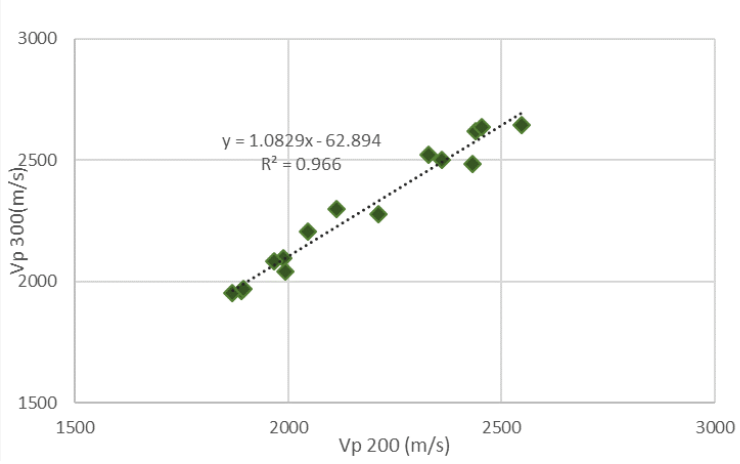

Figure 3.12: Influence of cement dosage on V_P

The results highlight that the waves speed increases by about 4-6 % when the cement dosage increases by additional 100 kg/m^3. This raise indirectly confirms that there is a greater amount of hydrates for soil cement mixtures with a higher content of cement.

The values of the dynamic modulus of elasticity calculated from the value of Poisson's ratio (ν= 0.3) are very different from the values of the modulus of elasticity calculated from the press data , so the values are not comparable. Each value represents the average value of 3 specimens.

S_2	E_{stat}(GPa)	E_{dyn} (GPa)
C_{200}	1.267	7.14
C_{250}	1.674	8.02
C_{300}	1.834	8.79

Table 3.9: Values of E_{stat} and E_{dyn} after 180 days of curing time

3.4 Durability

3.4.1 Sulphate attacks

The objective of this section is to understand the mechanism of sulphate attacks and study the effects of parameters related to this phenomenon.
In the soil mixing process, the contaminants and the other compounds, e.g. chlorides from saline water, are directly mixed with the injected binder and the soil. Hence, they are integrated into the soil mix matrix. As a result, the potential impact of these compounds is more important for the soil mix elements than for cast-in-place or precast concrete elements (only exposed to the contaminants along their contact zone with the ground). In this study a specific soil-concrete mixture with soil S_2 that incorporates 25 g/l of Na_2SO_4 was produced in order to investigate internal sulphate attacks. The water content remain the same as the other mixtures and the cement content is C_{150}. At the same time a mixture without sulphate was produced to compare the results.

Mass evolution

The Figure 3.13 shows the evolution of the relative mass of soil-concrete samples by comparing the samples with sulphate inside and those without. The results show that the mass of the samples ranges between $\pm$ 0.68% for sulphate specimens and $\pm$ 0.49 % for regular specimens. The specimens with the chemical agent present a fairly clear mass gain in relation to the intact specimens. The increase in sulphate sample mass is related to the precipitation of minerals such as ettringite (density of about 1.7 g/cm^3) and gypsum (density of about 2.3 g/cm^3) that fill partly the porous structure.

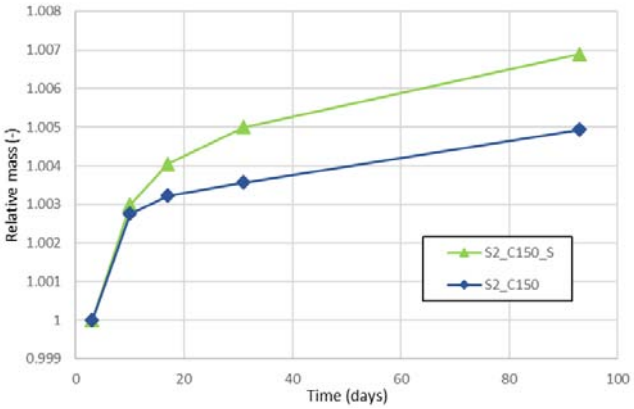

Figure 3.13: Evolution of relative mass versus time

Mechanical properties

Compressive strength The compressive strength are determined after 14, 28 and 90 days of curing time. The results show that sulphate affect the compressive strength and this difference is significant after 90 days of cure. The difference of strength after 90 days is about 1.8 MPa.

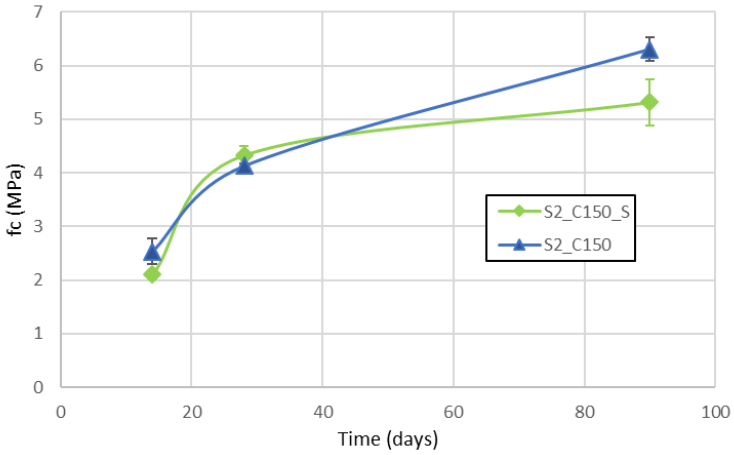

Figure 3.14: Evolution of compressive strength versus time for regular specimens and specimens with sulphate ($S2C_{150}$)

V_P measures Figure 3.15 shows the results of the evolution of wave speed over time. There is a slight increase of waves speed over time for both mixtures as a function of time. Non-destructive measures do not detect damages since no waves speed drop is observed by sulphate compounds. The use of CEM III/C with 85 % of slags which limits the amount of C_3A is the reason why it has a good performance to sulphate attacks. Although the phenomenon should be studied for a longer period of time to see the complete evolution that may change with the degradation of the material.

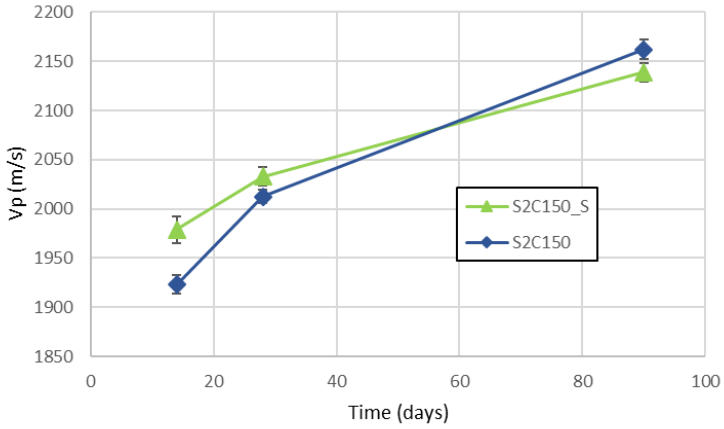

Figure 3.15: Evolution of wave speed versus time for regular specimens and specimens with sulphate ($S2C_{150}$)

3.4.2 Dimensional variations

A determination of the dimensional variations in water-saturated states was carried out. In practice, these tests are performed by measuring the kinetics of dimensional variations of concrete specimens sized 40x40x160 mm^3 using a retractometer , according to NF P 15-433, which offers a variation accuracy of10^{-3}mm. Results are expressed in terms of micrometer per meter.So the measure of the prismatic beam is taken after its demoulding to the day when its length remains practically unchanged.

Free swelling testing was performed for the soil-concrete mixture of S_2 with a cement content of 150 kg/m^3 until the age of 90 days.

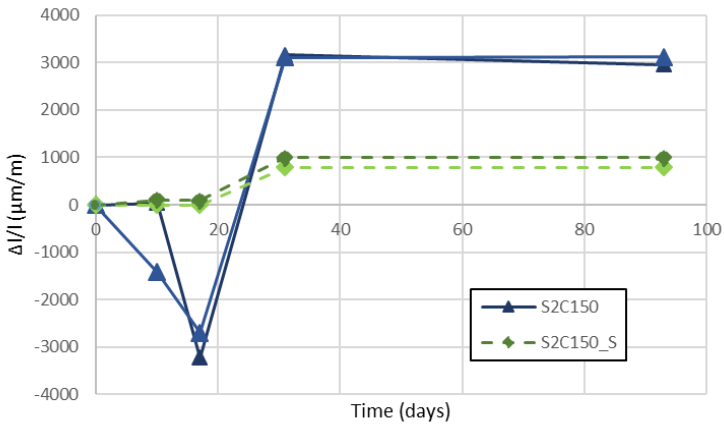

Figure 3.16: Dimensional variations after 90 days of curing time

3.4.3 Carbonation

In this study, the durability to carbonation of soil-cement mixture for soil S_2 with a cement content of 150 kg/m^3 and 200kg/m^3 was studied. The testing procedure provides that the samples initially saturated are exposed to normal atmospheric conditions. They were then stored in a room were the temperature and relative humidity (RH) is maintained at 20 degrees and 65% respectively. Under the natural curing conditions, the average measured CO_2 gas concentration in the room is $\simeq 0.03\%$.
Carbonation penetration was measured by spraying phenolphthalein indicator across the diameter of unsoaked samples after they had been tested in the unconfined compressive strength test. The phenolphthalein is colourless when the pH is lower than 8.2, but becomes pink beyond 9.9. The extent of carbonation could be clearly identified by the boundary of the colour change and the penetration from the outside towards the centre of the sample is measured in centimeters (cm) using a ruler. In fact, cement CEM III is composed of 85% slags (so the amount of Portlandite is minor), so the carbonation is much faster due to high porosity.

Figure 3.17: Carbonation depth of a soil-cement specimen subjected to a relative humidity of 65%

Four specimens S_2C_{250} (h=14 cm) were prepared in order to be exposed to carbonation. All of them were covered with a self-adhesive aluminum paper along the side surface but only two of them were also covered on the lower surface in order to evaluate the influence of moisture on carbonation. In fact the specimens are introduced into a plastic tray and submerged in water, leaving the upper surface exposed to air. The results of internal drying and carbonation depth are shown in the Table 3.10:

After 1 months, a carbonation depth around 1 cm was measured. Compared with conventional concrete, kinetics of carbonation is particularly high. This is due to the high porosity and permeability of soil-cement materials, which leads to a significantly faster drying and diffusion kinetics of CO_2 than conventional

S2C150	Internal drying (cm)	Carbonation depth (cm)
1	0.95 to 1.4	0.95
2	0.95 to 1.4	0.95
1f	0.95 to 1.55	1
2f	0.85 to 1.45	0.85

Table 3.10: Measure of internal drying and carbonation depth

Figure 3.18: Measure of (a) internal drying and (b) carbonation depth

concretes.
The results also show that there isn't a significant difference between the sample covered on the lower surface (1f and 2f in the table) and those which are not; but this aspect should be investigated for longer periods of carbonation.

In order to study the effect of cement dosage and level of RH on the carbonation of soil-cement materials, another test was carried out: 28 specimens (h=3 cm) of S_2 with a cement content of 200 kg/m^3 were manufactured in laboratory. Half of the specimens were totally dried and the other half were kept saturated. Then 7 chemical solutions (Table 3.11) were created in different containers in order to create different degrees of humidity. Four specimens (two dry and two wet) covered with a self-adhesive aluminum paper along the side surface were tested for each solution. The degree of humidity is kept constant thanks to air-tight containers.

The specimens were stored in a climatic chamber ensuring constant temperature (20 $\pm$ 2 $^\circ$ C) and taken out after 3 months. The final values derive from the average of 2 specimens for each type of moisture and for each degree of humidity.

Solution	Relative humidity (%)
Potassium nitrate	93
Potassium chloride	86
Sodium chloride	76
Ammonium nitrate	65
Magnesium chloride	33
Lithium chloride	12
Silica	3

Table 3.11: RH (%) for different solutions

Figure 3.19: Containers-RH (%)

These results show that the wet specimens are less subject to carbonation and around 76 % of relative humidity the values of carbonation depth are very low and reach zero for a relative humidity of 93 %. The figure shows that the depth of carbonation decreases linearly with the relative humidity (Figure 3.21).

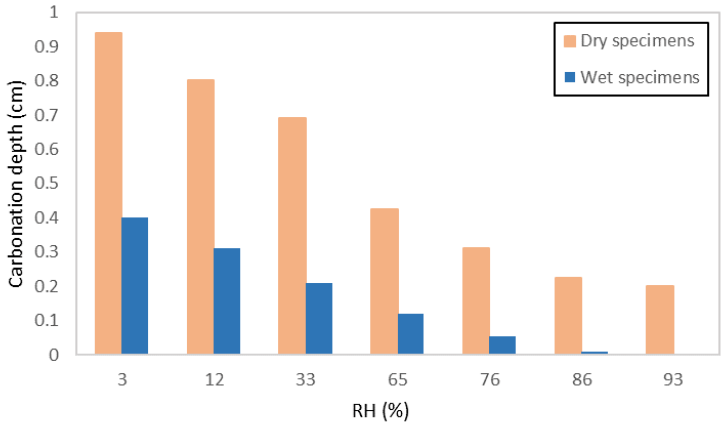

Figure 3.20: Carbonation depth and RH (%)

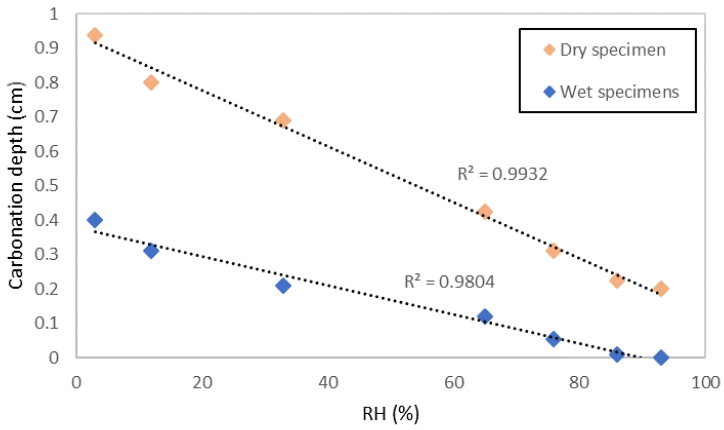

Figure 3.21: Carbonation depth and RH (%)

Compared to the results of the previous test we can assume that the carbonation depth decreases with the cement content increase up to 200 kg/m^3.

In general, the parameters influencing the carbonation of concrete samples are firstly, intrinsic parameters such as permeability, porosity (quantity and pores size) and cement content and secondly exposure conditions, such as relative humidity and CO_2 content. The increase of water content reduces the space available for the diffusion of CO_2 through the porous network of the cementitious matrix. However, carbonation reaction is favoured by the moisture content within pores and the carbonation reaction stops when the moisture in the pores of the material becomes insufficient to allow the CO_2 dissolution. Therefore, depending on porous network, there is a relative humidity and water content for which the carbonation reaction is optimized.

3.5 Behavior at high temperature

This section presents the results for the specimens of soil-mix concrete subjected to high temperature in order to investigate their behavior at high temperature. This kind of accidental events of fire may occur for example when soil-mix concrete is used for the construction of retaining wall in underground parking.
The research work presents firstly the results of identification by TG and TD analyses; the evolution of mass loss as a function of temperature and then the residual mechanical properties are determined at the same temperatures (compressive strength,static and dynamic elasticity module).

3.5.1 Thermogravimetry and Differential thermal analyses

The thermogravimetry and differential thermal analyses are used for identifying the different losses and physic and chemical transformations occurring during heating of the material. The test were carried out on dry samples, thereby the evaporation of free water is not considered. The diagram of TDA (Figure 3.23) has two endothermic peaks : one between 100 and 200 °C due to the loss of water originally present in the inter-layers of the clay and the second at 750 °C derives from the removal of hydroxyls. This is a typical behavior of a *Montmorillinite* clay as we can see in the Figure 1.7 [15] and the presence of clay is confirmed by the results of the grain size analysis which highlights the large amount of clay present in the soil.This second endothermic reaction causes a structural change which makes the clay reactive with lime.

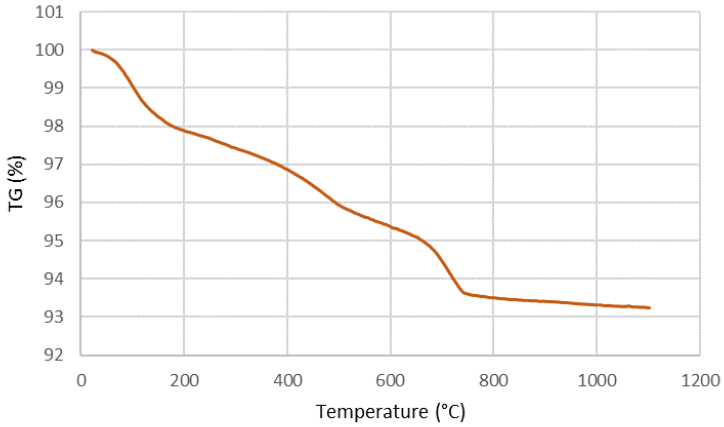

Figure 3.22: TGA results for soil S_2

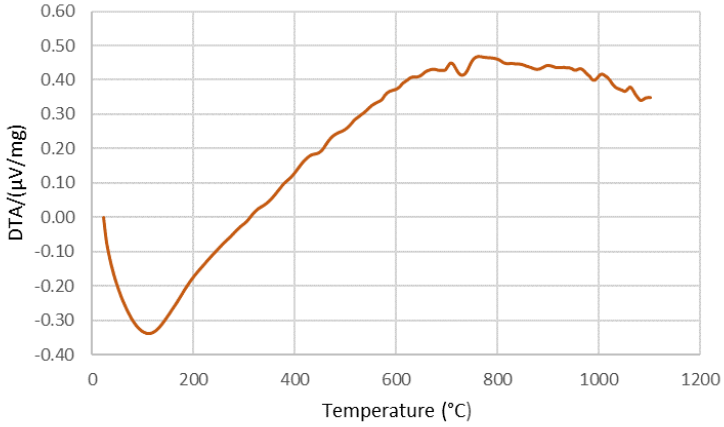

Figure 3.23: DTA results for soil S_2

The thermogravimetry analysis (Figure 3.22) shows in correspondence of the two endothermic peaks of the DTA two weight losses.
These transformation are also observed for the soil-cement material in the same temperature ranges . In the next figures (Figure 3.24 and 3.25) we can see the comparison between the analyses carried out for soil-cement samples with a cement dosage of 250 kg/m^3,in particular for samples taken at room temperature and for samples taken after heating at 300 and 850 °C.

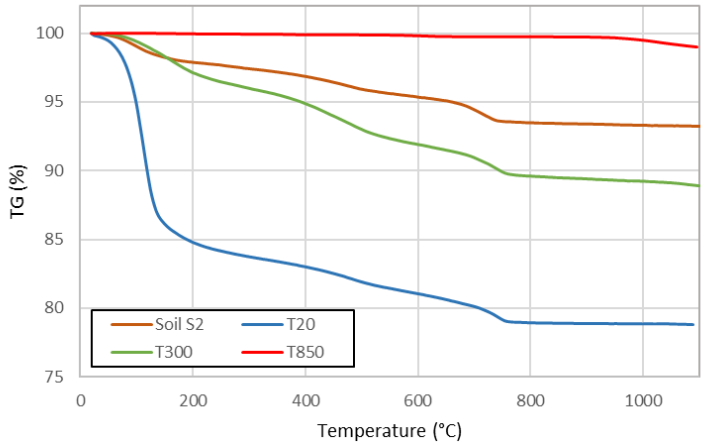

Figure 3.24: TGA for soil S_2 and specimens C_{250} at different temperatures

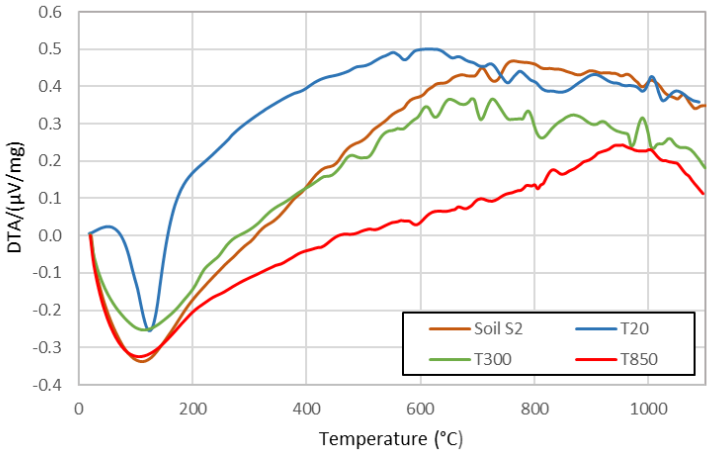

Figure 3.25: TDA for soil S_2 and specimens C_{250} at different temperatures

It is clear that the specimens subjected to higher temperature, after a TGA test, show a minor mass loss due to the minor water content inside. Compared to the previous case there is in addition the transformations related to the presence of the cement. At first around 100 °C there is the loss of the physically bound

water to the soil-cement matrix and then it starts the dehydration of the silicate gel hydrates (C-S-H) followed by a peak due to the decomposition of calcium carbonate between 750 °C and 850 °C where $CaCO_3$ decomposes into CaO.

3.5.2 Thermal response

The characterization test until 850 °C of heating has been carried out employing three specimens (d=6cm;h=12cm) for each concrete dosage and for soil S_2. A thermocouple was inserted inside and on the surface of the specimen for each mixture in order to evaluate the trend of temperature during the tests, as shown in Figure 3.26.

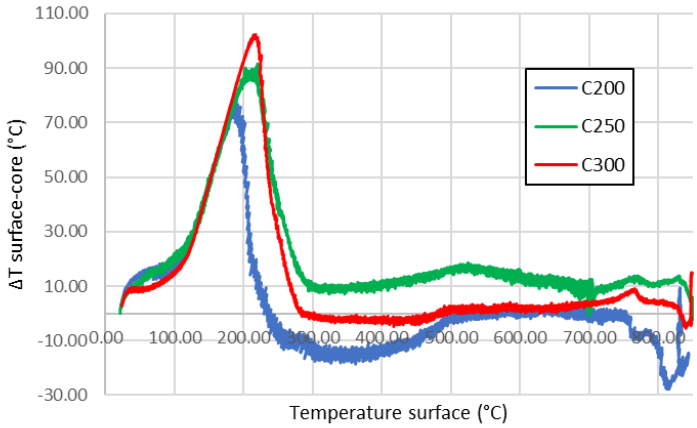

Figure 3.26: Thermal response of soil-concrete specimens

The behavior of soil-concrete material is almost the same for the three different mixtures, but there is a difference of peak value which usually represents physical and chemical changes, such as the C-S-H dehydration ,water evaporation and crystalline transformations. Usually the positive ΔT peak between the temperature on the surface and the temperature of the specimen's core is due to an endothermic reaction of concrete which consume heat, on the other hand the negative peaks of ΔT are due to an exothermic reaction which produce heat.
The increase of the peak is decelerated between 50 and 100 °C reflecting a higher conductivity of the material. The high consumption of heat related to the large amount of free water in latent form increases the inertia of the material and the heat diffusion is slower than for normal concrete; improving the thermal protection of the material[17].

Mixture C_{200} has a peak with a lower amplitude in comparison with mixture C_{300} and that is why the amount of free water added for soil-concrete mixture with a larger amount of cement is higher in order to reach a water content of 50 % (Table 2.4).

Mixture S_2	Δ T (°C)	T surface (°C)	T core (°C)
C_{200}	78.4	189	108.2
C_{250}	91.6	221	129.5
C_{300}	102.3	217	115.1

Table 3.12: Core and surface temperature of specimens

One also notices faster descent of the temperature shift after the peak in the case of mixture C_{200}; in fact the heat consumed by the decomposition of C-S-H which starts once the free water is gone, is higher for mixture C_{300} and thus lead to a gradual decrease of temperature shift (Figure3.27).

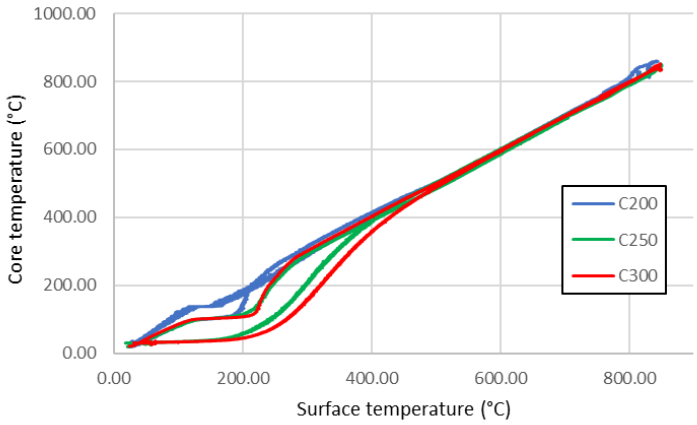

Figure 3.27: Surface temperature versus core temperature

3.5.3 Physical and mechanical properties at high temperatures

Mass Loss

The mass of 3 specimens has been measured for each cement dosage mixed with soil S_2 . Figure 3.28 shows the loss in mass in function of the temperature. The results show that the loss of mass increases with the temperature and that a major cement content leads to a minor loss in mass for the specimens. The loss of

mass measured between the value at room temperature and the value obtained after the heating phase at 300 °C for all mixture is due to the loss of the free water, the adsorbed water and bound water and that is the reason why we can observe a significant loss of mass in this range of temperature (Figure 3.28).

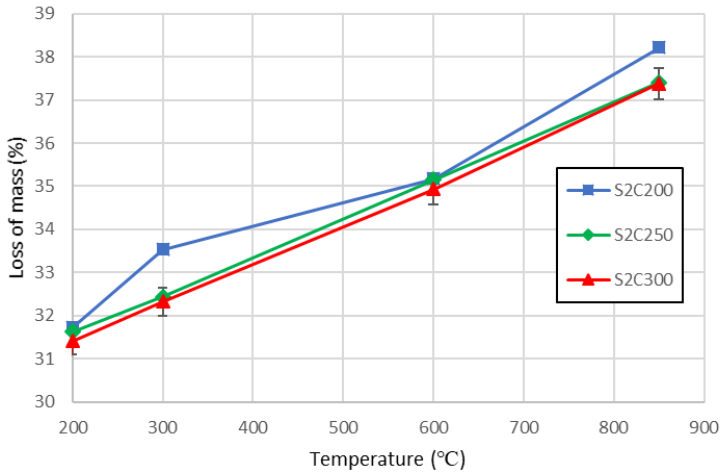

Figure 3.28: Relationship between loss of mass on initial mass versus temperature

For ordinary concrete this significant loss is observed between 150 and 300 °C and its related to the loss of free water initially confined in C-S-H. In the case of soil-concrete material the loss is already significant from a temperature of 60 °C as a result of the large amount of initial free water due also for the method of conservation.

Reached the temperature of 200 °C the increase is less relevant and became almost constant as a function of the temperature. This sudden change is due to the difference of the type of water released during the test. The mass loss related to the dehydration of the C-S-H (between 60 and 300 °C) is low compared to that one related to free water and to the water present in the interlayers of the clay; this is connected to the particular composition of soil-concrete material with a ratio W/C way above the ratio needed to the hydration of the cement mass. After 600 °C there is another increase of loss due to the second phase of C-S-H dehydration.

The same relation can be traced calculating the loss mass in relation to the dry mass after the heating tests in order to highlight that the mass loss is related to water content of mixing water (%).

Mixture	S_2C_{200}	S_2C_{250}	S_2C_{300}
Water mixing (%)	50	50	49.9
Mass loss at 850 °C (%)	62	59.7	59.77

Table 3.13: Comparison between water content of mixing water and mass loss after heating at 850 °C

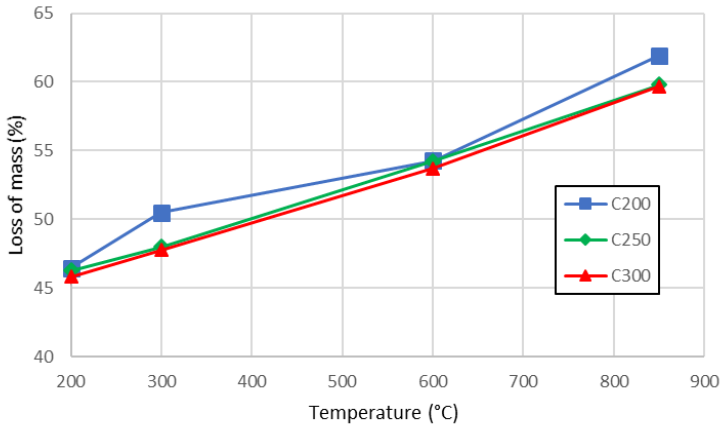

Figure 3.29: Relationship between loss of mass on final mass versus temperature

Behavior of compressive strength of concrete with temperature

The Figure 3.31 shows the compressive strength variation depending on the temperature. The results are also normalized from the value of strength obtained after 180 days of curing time. The compressive strength drops drastically already at 200 °C and a slight recovery occurs at 300 °C, especially for the mixture C_{300}.So after exposure to 300 °C, the specimens showed an improvement in residual compressive strength compared to that measured after exposure to 200 °C. This phenomenon has been observed by several authors and has sometimes been interpreted as a consequence of CSH re-hydration at 300 °C, when water migrates and condenses within the colder areas of the sample [16]. Then the value of strength descends up to 850 °C where is close to zero.

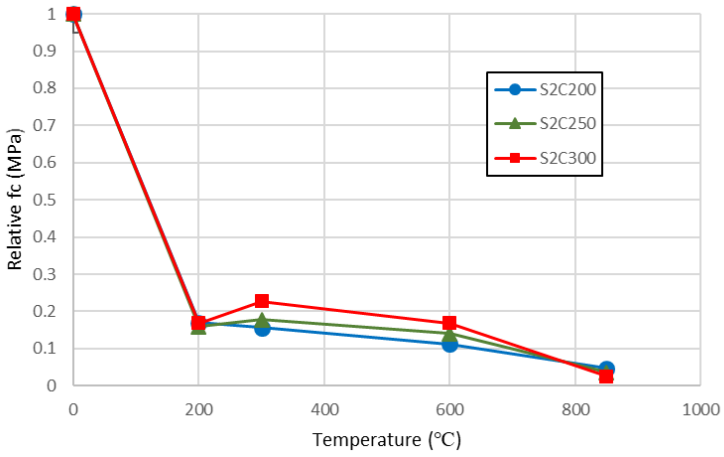

Figure 3.30: Relationship between relative compressive strength versus temperature

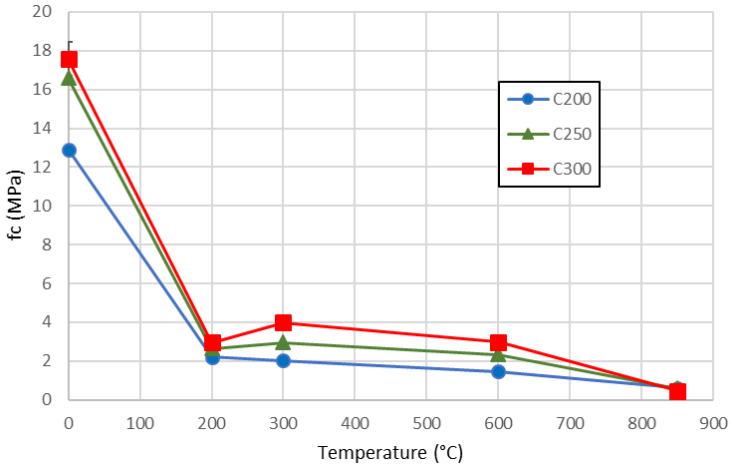

Figure 3.31: Relationship between compressive strength versus temperature

Temperature (°C)	fc C_{200} (MPa)	fc C_{250} (MPa)	fc C_{300} (MPa)
20	12.9	16.6	17.56
200	2.2	2.64	2.95
300	2	2.94	3.99
600	1.45	2.33	2.96
850	0.61	0.65	0.44

Table 3.14: Compressive strength values with temperature variations

The next figures represent the stress-strain curves for the different mixtures of soil-concrete.

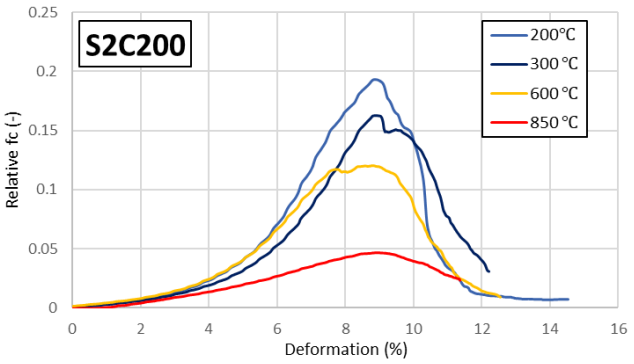

Figure 3.32:
Stress-Strain curves after heating tests - C_{200}

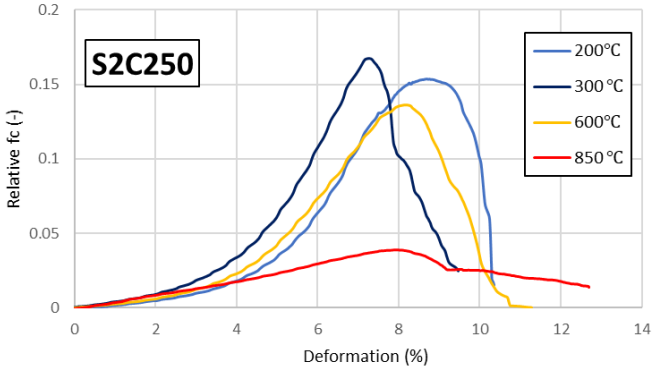

Figure 3.33:
Stress-Strain curves after heating tests - C_{250}

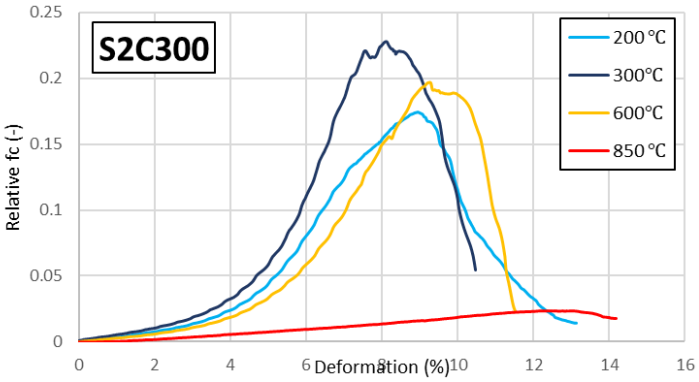

Figure 3.34:
Stress-Strain curves after heating tests - C_{300}

Modulus of elasticity

The figure 3.36 shows residual elastic properties of soil-concrete material subjected to heating (200,300,600, 850 °C). The dynamic modulus is calculated from the P-waves speeds and density of the specimens after the heating tests using a Poisson's coefficient of 0.3. A drop of about 60 % in the dynamic modulus of elasticity is recorded for all mixtures between 20 and 200 °C and about 80 % at 300 °C . This drop is much more significant than that of structural concrete (f_c=38MPa) whose Young's modulus decreases by only 35 % after a thermal history at 300 °C [19]. At 300 °C the value is between 1.48 and 2.8 GPa then at 600 °C there is a slight increase, especially for C_{200} specimens, and the modulus reaches about 3 GPa.This gain can be explained by the fact that around 135-350 °C occurs the dehydration of C-S-H so after this range between the strips of C-S-H compounds there is no more available water, so this can lead to the union of the strips and an increase of the dynamic modulus. At 850 °C the specimens were too damaged to make measurements.

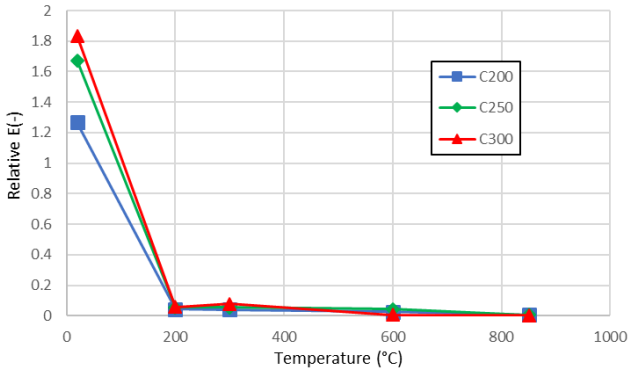

Figure 3.35: Evolution of modulus of elasticity as a function of temperature

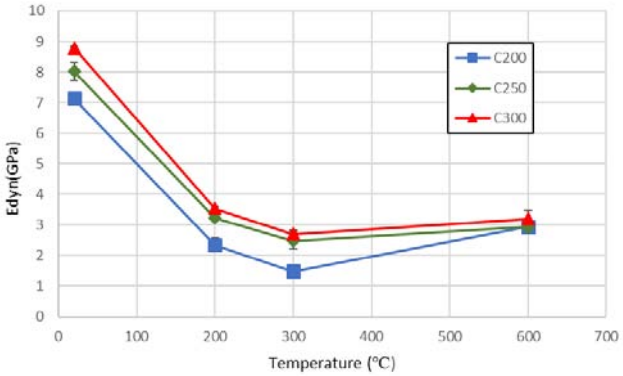

Figure 3.36: Evolution of dynamic modulus of elasticity as a function of temperature

Visual observations

In this section some images of the specimens after thermal history are shown in order to investigate the damages on specimens. At high temperatures it occurs an internal distribution of stresses that cause cracks, due to different expansion coefficients for the presence of different materials inside the soil cement mixture. There is a change in the volume of the structure that leads to a cracking state increasing with temperature. In fact the figures show that there are more cracks when the specimens are subjected to higher temperatures and for mixtures with a lower cement dosage. It is interesting to see the color difference between the heating at 300 °C and 850 °C and this is due to the removal of hydroxils of the Montmorillinite at 750 °C. These effects on the specimens confirm the results of the test of mechanical properties after the heating history.

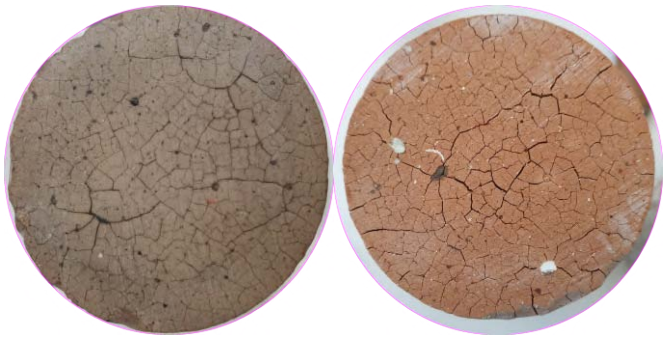

(a) **(b)**

Figure 3.37: Cracks on C_{200} specimens at a) 300 °C and b) 850 °C

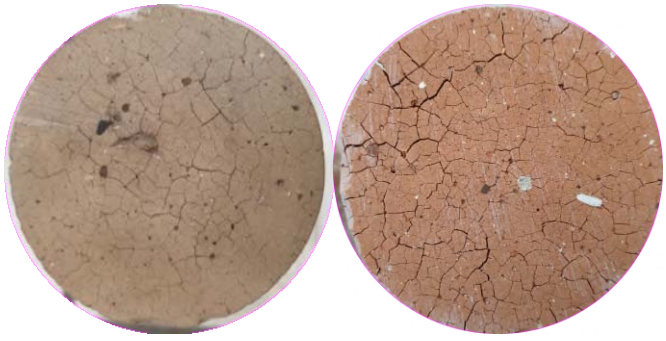

(a) **(b)**

Figure 3.38: Cracks on C_{250} specimens at a) 300 °C and b) 850 °C

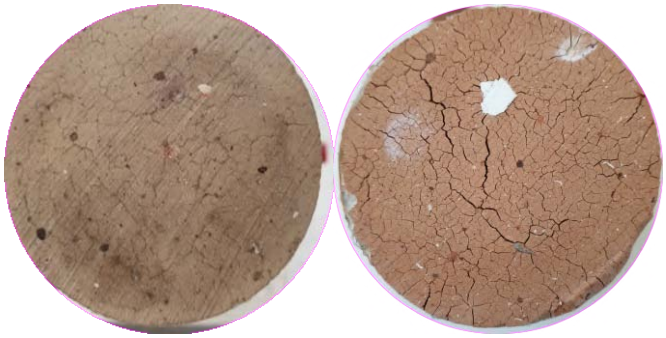

(a) **(b)**

Figure 3.39: Cracks on C_{300} specimens at a) 300 °C and b) 850 °C

So after 850 °C there is no more resistance and cohesion left and the specimens break very easily. Calcination gives to the soilcrete specimens a whitish colour on the surface.

Figure 3.40: Specimens after 850 °C

Chapter 4

Geotechnical Applications

In this last chapter some examples of applications of DMM are presented, in order to demonstrate how the technique can improve in general the stability and safety of earth structures. Especially the stability of embankment is investigated through a simulation with the software *Geostudio* after the application of soilcrete walls as reinforcement; then some case studies are described in order to see how soilcrete material can be used for remediation of contaminated soils and as retaining structures.

4.1 Effects of Deep Mixing Method to reinforce earth levees

Sliding and internal erosion due to floodwater or piping are two key factors causing earth levees' failures. The method of Deep Mixing Method (DMM) can be proposed to reinforce earth levees. The DMM creates a soil cement wall having better engineering properties such as higher strength and low hydraulic conductivity than those of the in-situ soils. The study investigates capacity of the DMM to reinforce earth levees in against annual floods. Seepage and slope stability analyses under various conditions were performed with various scenarios of earth levee's body.

4.1.1 Limit Equilibrium

Limit equilibrium types of analyses for assessing the stability of earth slopes have been in use in geotechnical engineering for many decades. The idea of discretizing a potential sliding mass into vertical slices was introduced early in

the 20th century and is consequently the oldest numerical analysis technique in geotechnical engineering. Many different solution techniques for the method of slices have been developed over the years. Basically, the methods are all very similar. The differences between the methods are depending on what equations of statics are included and satisfied and which interslice forces are included and what is the assumed relationship between the interslice shear and normal forces. Figure 4.1 illustrates a typical sliding mass discretized into slices and the possible forces on the slice. Normal and shear forces act on the slice base and on the slice sides.

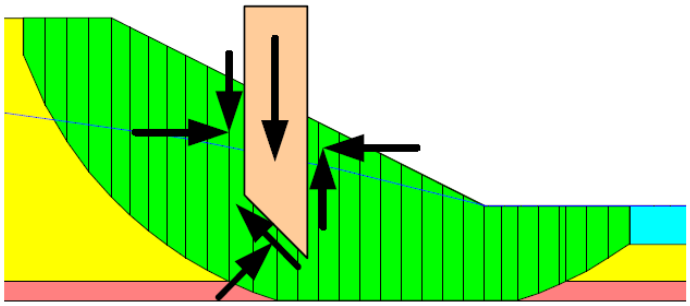

Figure 4.1: Slice discretization and slice forces in a sliding mass

Morgestern-Price Method Morgenstern-Price is a general method of slices developed on the basis of limit equilibrium. It requires satisfying equilibrium of forces and moments acting on individual blocks. The blocks are created by dividing the soil above the slip surface by dividing planes. Forces acting on individual blocks are displayed in the following figure:

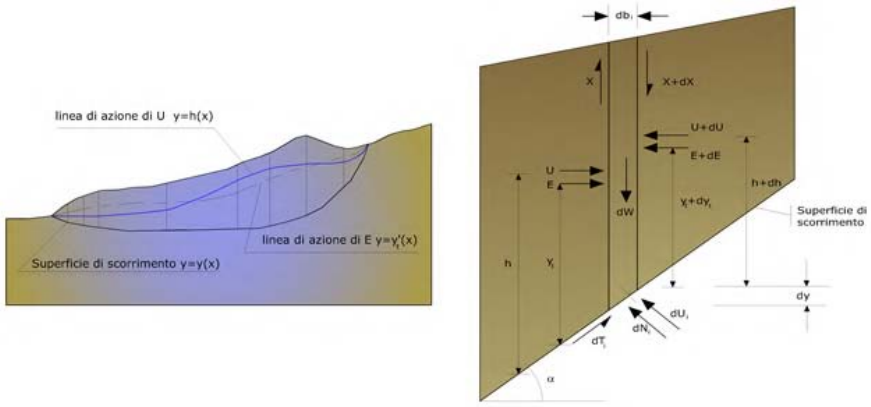

Figure 4.2: Forces in a sliding mass and representation of a generic slope

This method uses two factor of safety equations; one with respect to moment equilibrium and another with respect to horizontal force equilibrium. He adopted a constant relationship between the interslice shear and normal forces, and through an iterative procedure altered the interslice shear to normal ratio until the two factors of safety were the same. Finding the shearnormal ratio that makes the two factors of safety equal, means that both moment and force equilibrium are satisfied. The following equation relates the interslice shear (X) and normal (E) forces.

$$X = E\lambda f(x) \tag{4.1}$$

Where λ is a factor of scale reflecting the percentage of the function required to satisfy the equilibrium of the forces and moments, while the function f(x), function of the position of E and X, defines a relation between the variation of the force X and force E inside the sliding mass, i.e the inclination of the resultant interaction forces along the sliding surface. This function can be chosen arbitrarily (constant, half sine, sinusoid,etc). The Factor of Safety for the Method of Morgestern-Price is identified from the meeting point between the two curves, so both moment and force equilibrium are satisfied.

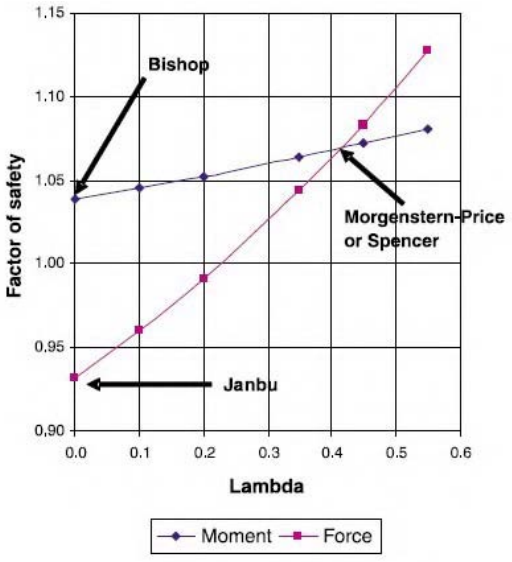

Figure 4.3: FS- λ

In summary, the Morgenstern-Price method:

- Considers both shear and normal interslice forces;
- Satisfies both moment and force equilibrium;
- Allows for a variety of user-selected interslice force function

4.1.2 Geostudio

The finite element based software *Geostudio 2019* is specific for the study stability of earth structures and that gives the possibility to outline different scenarios and to analyse numerous dynamics and critical points of a project related to natural and artificial soils. The software allows to perform analysis such as stress-strain, seepage, slope stability, dynamic analysis. The two analyses considered in this study are respectively:

Slope Stability Analysis Factor of Safety (FS) is used to evaluate sliding of an earth levee. In this study, the Morgestern-Price method was employed to determine FS. Theoretically, if a FS is greater than 1.0, an earth levee is safe with sliding, and vice versa. A FS is defined as a ratio of resistance moment to driven moment based on the Limit Equilibrium Theory.

$$FS = \frac{ResistantMoment}{DrivenMoment} \tag{4.2}$$

As shown in Figure 4.4 it is necessary to solve the forces equilibrium of the slices in order to calculate the value of the Factor of Safety. The determination of this value need some assumptions in order to simplify the problem, otherwise there are too many variables and the system of equation results indeterminate. Generally the assumptions are that the resultant of the actions at the base of the slice is centered on the center line and the forces between the slices are neglected. The equation is the following :

$$FS = \frac{(\sum_{i=1}^{n}(W_i cos\alpha_i - u_i l_i)tan\phi'_i + \sum_{i=1}^{n} c'_i l_i)}{\sum_{i=1}^{n} W_i sin\alpha_i} \tag{4.3}$$

where

- c' - Cohesion;

- ϕ'- Internal friction angle;
- W_n - Weight of slice;
- u – Pore water pressure at the base of slice;
- α_n – angle of a slice base to horizontal.

Figure 4.4: Parameters of a slice

The Slope/W software was used to determine FS. This analysis investigate the possible failure mechanisms of the part of the patch of soil considered through the Limit Equilibrium Method.

Seepage The flow of water through soil is one of the fundamental processes in geotechnical and geoenvironmental engineering. SEEP/W ,a subproduct of *Geostudio*, is a finite element software which can simulate the movement and pore-water pressure distribution within porous materials like soil and rock, so it can mathematically simulate the real physical process of water flowing through a particulate medium.
The general governing equation for 2D seepage is shown in Equation (4.4). In the case of steady-state condition, the flux entering and leaving a unit volume is constant, and the right hand side of Equation (4.4) is neglected to become equation (4.5).

$$k_x \frac{\partial^2 H}{\partial x^2} + k_y \frac{\partial^2 H}{\partial y^2} + Q = \frac{\partial \theta}{\partial t} \tag{4.4}$$

Steady-state condition

$$k_x \frac{\partial^2 H}{\partial x^2} + k_y \frac{\partial^2 H}{\partial y^2} + Q = 0 \tag{4.5}$$

where

- k_x, k_y hydraulic conductivity in x,y direction respectively;
- H - Total head difference;
- Q - applied boundary flux;
- θ - Volumetric water content and t - time.

The software *Seep/W* was used for seepage analysis where the filtration processes among the soil quantitatively and in terms of time is investigated; considering the physical characteristics of the materials. The geometric base is suitably modelled for both analyses and the results are common for both analyses in order to considerate all the events that can possibly occurs. So the analyses can be evaluated separately or together in the case where the processes affect each other.

Case study

The next figure presents the embankment considered for the study and to which stability and filtration analyses have been applied. The input data given to the software are the embankment geometry and its material properties.

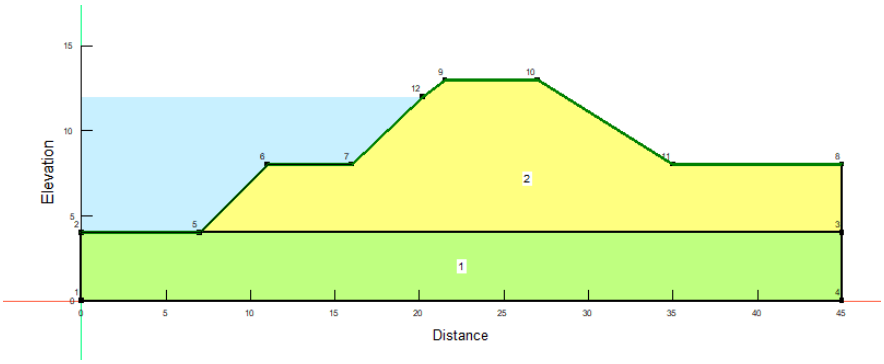

Figure 4.5: Section of the earth levee (1) Sand (2) Sandy Loam

Material	γ_{sat}(kN/m^3)	$\phi(\circ)$	$c^{'}(KPa)$	C_u(KPa)
Sand	19	32	8	-
Sandy Loam	19,5	23,04	4	32,14

Table 4.1: Properties of materials

The embankment consists of two layers with different materials and the properties of these materials are shown in the following table.

The aim of this study is to see the difference between a levee with no reinforcement and a levee after a reinforcement. The reinforcement is applied using Deep Soil Mixing Method through soilcrete walls and the properties of soil mixing material are obtained thanks to the laboratory tests outlined in the previous chapters. (Tab 4.2).

Permeability (m/s)	S_2C_{200}	γ_{sat}(kN/m^3)	$\phi(\circ)$
1,4 $\cdot 10^{-11}$		16,8	36

Table 4.2: Soilcrete properties for simulations

Data refer to soil S2 with a cement dosage of 200 kg/m^3. The soilcrete walls were assumed to build along the earth levee length.

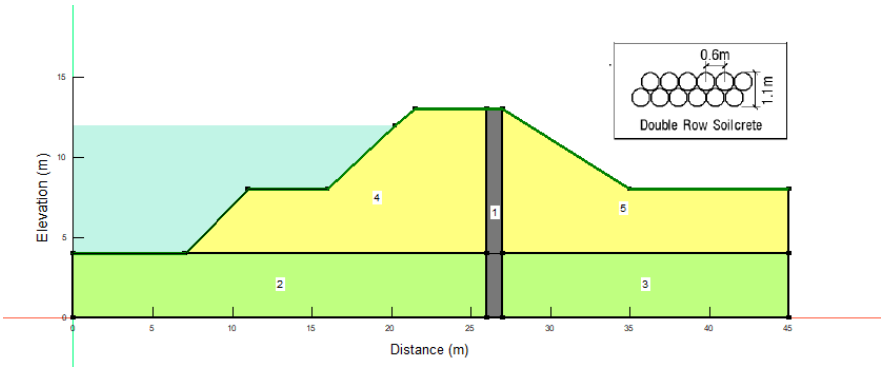

Figure 4.6: Levee with (1) soilcrete wall for reinforcement

Internal friction angle ϕ and cohesion c of soil-cement mixture [20] Researches on the strength properties of soil-cement mixture started as early as the 1950s. Based on triaxial shear tests, Balmer [21] firstly found that the internal friction angle ϕ of soilcement mixture stayed constant roughly regardless of the cement content. The value of the internal friction angle ϕ is 36 °C for

fine grained soil-cement mixture and 43 °C for granular soil-cement mixture. To study the effect of testing methods and verify the previous research findings, a series of laboratory tests on silt-cement specimens with a dosage of approximately 20 % cement by weight were carried out. Their testing results showed that the range of internal friction angle ranges approximately from 32 to 38 °C , which is close to the findings of Balmer [21]. Contrary to the findings aforementioned,other testing results obtained indicated that the internal friction angle ϕ is not relatively constant, and it varies in a similar fashion as the cohesion c as a function of the cement dosage, soil type, and curing condition and time. Balmer also found that the value of cohesion c of soil-cement mixture ranges from approximately 35 psi (241 kPa) to 530 psi (3654 kPa) depending on the cement dosage and the soil type. Mitchell [23] recommended that the cohesion of soilcement mixture can be estimated by

$$c = 48,265 + 0,225q_u \tag{4.6}$$

where the UCS q_u is expressed in kPa. The above review showed that the strength parameters of soil-cement mixture are influenced by many factors. It seems that the cohesion c increases when q_u increases, while the internal frictional angle f is relatively stable: 32 e 36 for fine-grained soilcement mixture and 38 e 43 for coarse-grained soil-cement mixture. These values are important because the effective concept of c and ϕ is necessary in this study.

Other shear tests on soilcrete material were conducted and performed at normal stresses of 50 kN/m^2, 100 kN/m^2 and 200 kN/m^2 up to a total shear displacement of 18 mm [22]. The effect of cement content on shear strength is plotted and peak strength envelopes and the development of cohesion and friction angle are respectively compared. Figure 4.7 illustrates the MohrCoulomb failure envelopes for peak strengths of untreated and cement stabilized soil at different cement contents.
The obtained values of peak strength parameters cohesion c and friction angle ϕ are extracted in figure 4.8. Figure 4.8 presents also the corresponding peak friction angle and cohesion vs. cement ratio. It is clear that the cement stabilisation significantly improves the shear strength of clay soil. The results show that there is an increasing in both cohesion and peak friction angle value. Nevertheless the cohesion tends to increase considerably non linear with increasing cement content and the peak friction angle reaches high values by small cement contents.

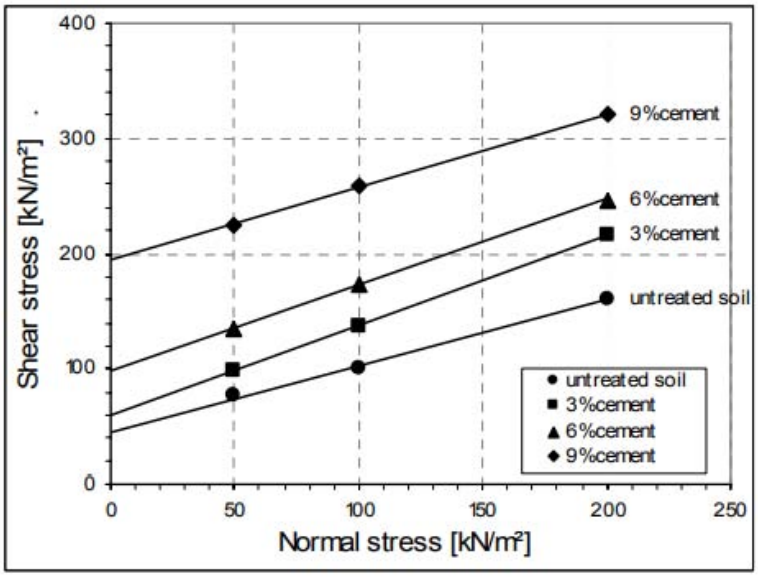

Figure 4.7: Peak strength envelopes of soil-cement-mixture

Cement ratio by weight [%]	Peak parameters	
	Angle of internal friction φ [°]	Cohesion c [kN/m²]
Untreated soil	29.7	46
3%	38.5	57
6%	36.8	98
9%	32.5	193

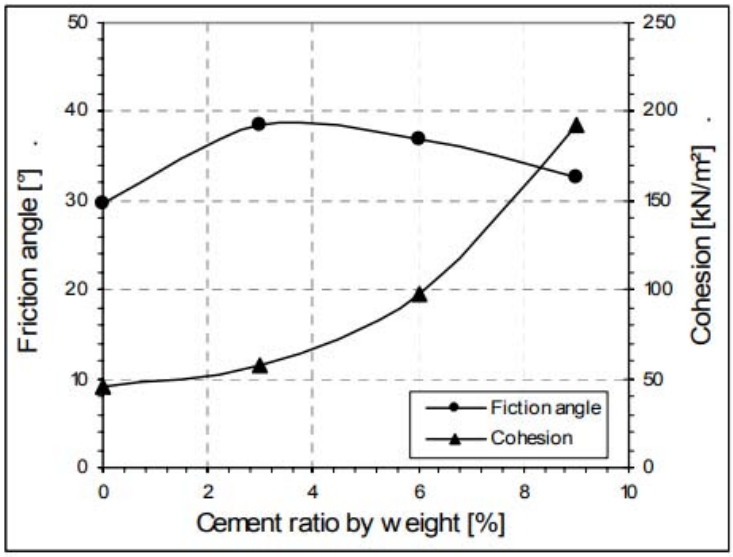

Figure 4.8: Shear strength parameters and Peak friction angle and cohesion vs. cement ratio

4.1.3 Results

Seepage

Thanks to this analysis it is possible to obtain the phreatic line and to investigate the stability taking into account the highest floodwater, considering a reservoir level of 12 meters. This analysis requires the definition of the hydraulic boundary conditions. The water total head represents the reservoir level (12 m in this case) and on the other side of the levee the level is assumed to be in zero pressure conditions, i.e in equilibrium condition with atmospheric pressure and along the downstream side of the embankment is applied the drainage condition to allow water to exit the domain if the pressure exceed 0 kPa. One of the main differences between the two cases, with and without reinforcement, is identified by the phreatic line, as figure 4.10 shows. It can be seen that the soilcrete walls work well in term of seepage flow cut off.

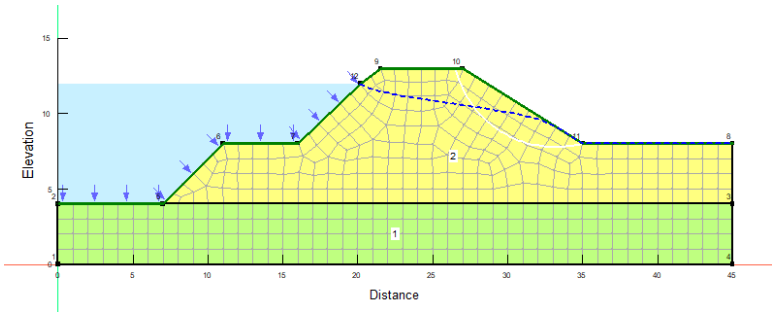

Figure 4.9: No reinforcement-Phreatic Line

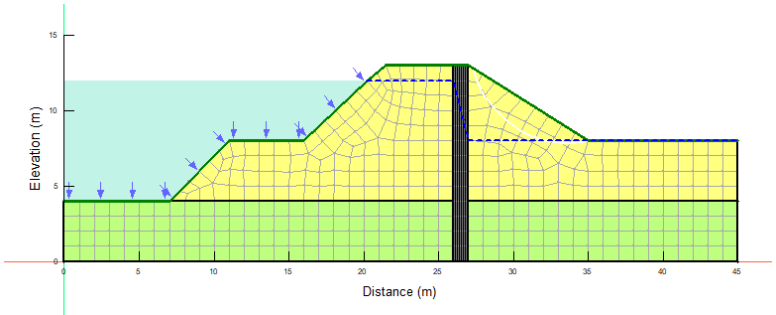

Figure 4.10: Soilcrete wall for reinforcement-Phreatic Line

In SEEP/W an important variable is the total hydraulic head, which is made up of pressure head and elevation. The elevation represents the gravitational component. Contours of total head are the equivalent of equipotential lines. In equation form the total head is defined as :

$$H = \frac{u}{\gamma_w} + y \tag{4.7}$$

where:

- H - the total head (meters),
- u - the pore-water pressure (kPa),
- γ_w - the unit weight of water (kN/m^3),
- y - the elevation (meters).

The term $\frac{u}{\gamma_w}$ is referred to as the pressure head, represented in units of length. In the next figures there is the difference of the distribution of water total head before and after the reinforcement.

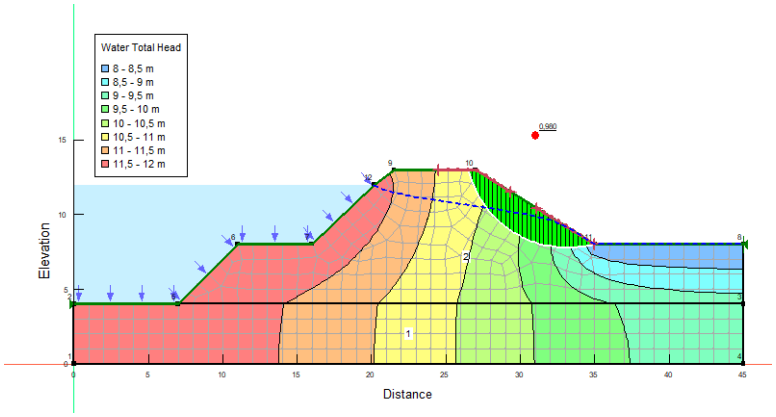

Figure 4.11: No reinforcement-Water Total Head

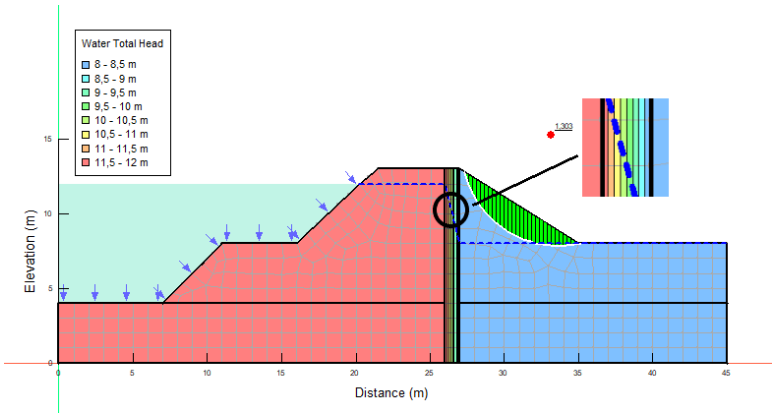

Figure 4.12: Soilcrete wall for reinforcement-Water Total Head

Also the water flux for the two different cases can be represented (Figure 4.14 and 4.13).

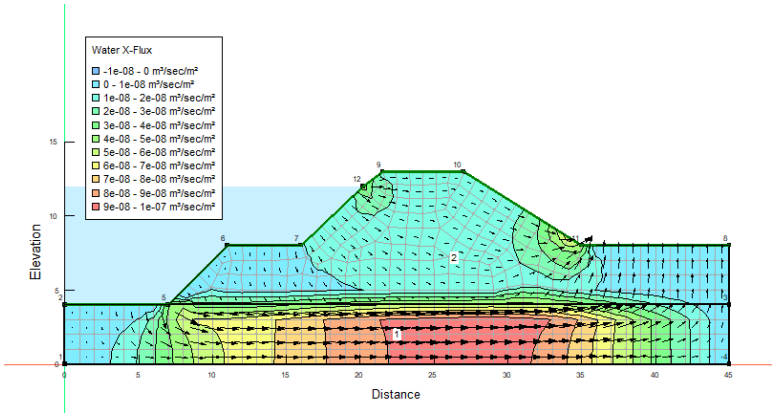

Figure 4.13: No reinforcement-Water Flux

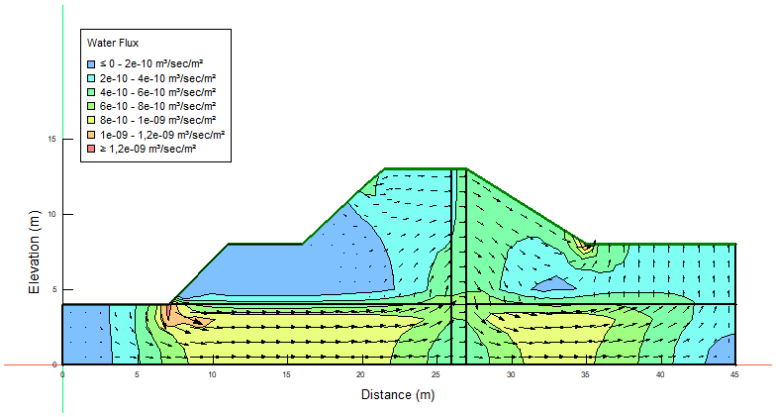

Figure 4.14: Soilcrete wall for reinforcement-Water Flux

The soilcrete walls significantly reduce the maximum water flux, slowing down to 1,2 e^{-09} m/s (from 1 e^{-07}) through the middle of the sandy base and the output/input section respectively for the levee without reiforcement and with soilcrete walls. This reduction is due to lower permeaiblity of the levee thanks to the presence of the soilcrete walls. Due to its very low permeability after the reinforcement the soilcrete walls reduce the value of the water flux, which decrease almost to zero. Normally an high seepage quantity can wash soil particles along holes inside the earth levee body and may break some section of an earth levee under floodwater pressure and this is a typical failure of earth levees.

4.1.4 Slope Stability

The results of stability analyses show that the reinforcement through soilcrete walls increases the Factor of Safety from 0,98 to 1,303 making the earth levee safe.

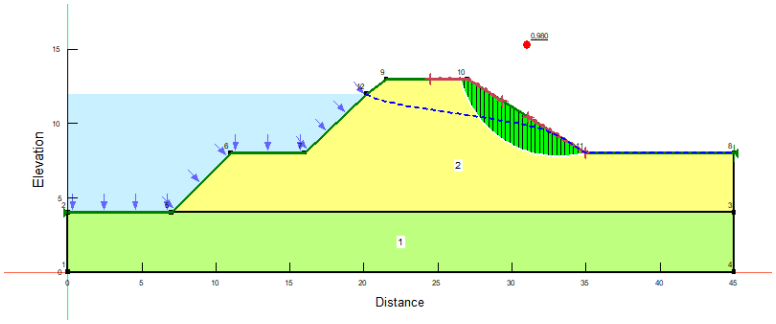

Figure 4.15: No reinforcement-Slope stability analysis

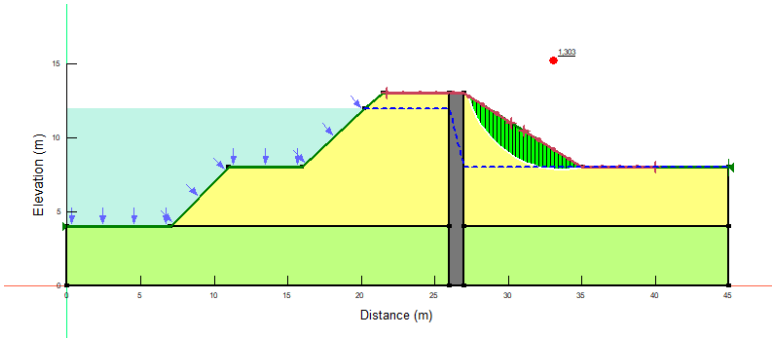

Figure 4.16: Soilcrete wall for reinforcement-Slope stability analysis

Piping analysis The phenomenon of piping is the process of retrograde internal erosion in sandy layers underneath clay/loamy levees and due to high seepage flow during the flood season is the main reason to cause earth levee broken under floodwater pressure. Therefore, an appropriate soilcrete wall system can reinforce earth levees to cutoff seepage and prevent piping effectively.

The process starts with heave and cracking of the soft soil top layer at the land side of the levee, caused by high water pressures which are easily transferred through the permeable sand layer (Figure 4.17a-b). The cracks in the top soft soil layer allow for seepage. In case the water level difference between river and land side (the hydraulic head) is large enough, sand grains may be transported along with the water flow, thereby creating a pipe underneath the levee (Figure 4.17c-d). Continuing erosion may finally lead to failure of the levee and break-

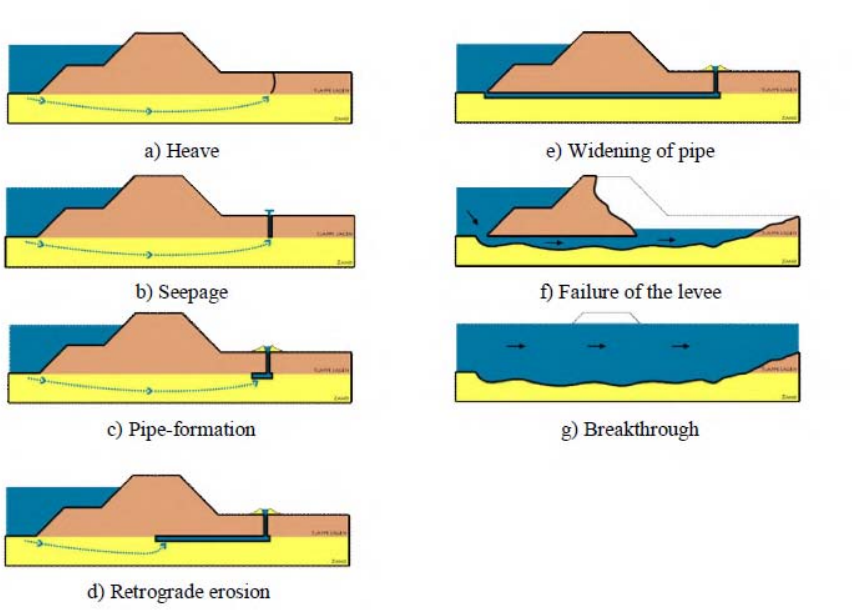

Figure 4.17: Process of retrograde erosion

through (Figure 4.17e-g).

This occurrence is related to the presence of seepage flows from the ground upwards.This flow induces on the soil grains dragging forces and the effect can be pushed to the point where the effective tensions become zero; in this case the soil behaves like a fluid and therefore is no longer able to withstand shear stresses. In order to study this process the critical gradient is compared with the hydraulic gradient down over the ground level.
The critical gradient is calculated as follow :

$$i_c = \frac{\gamma_{sat} - \gamma_w}{\gamma_w} \tag{4.8}$$

The hydraulic gradient is calculated as :

$$i = \frac{\Delta H}{L} \tag{4.9}$$

where ΔH is the total head difference over the ground level, L is the seepage path through the section in question. In order the avoid the phenomenon of piping i must be less than i_c (i $< i_c$)

There is another way to improve the stability of an embankment. In fact embankments founded on deep mixed soil-cement column reinforced soft ground results in enhanced bearing capacity and reduced settlements. The extent of improvement in stability and settlement characteristics of embankments founded on deep mixed column improved ground mainly depend up on the properties of DM columns, column spacing and column diameter. Structures founded on soft organic clays have high probability of foundation failures such as bearing capacity failure and excessive settlement. With growing need for infrastructural developments it is necessary to construct various structures on soft grounds also. Hence various techniques are used to improve the soft ground and safely construct over it. Most widely used techniques for improving soft soil deposits are preloading, stone columns, deep mixing, mass stabilization and rigid piling. Deep mixed soil-cement columns are used for improving soft organic clay extending to great depths especially when the construction has to be speeded up and when differential settlements with respect to the adjacent structure are to be restricted. DMC columns are widely used for supporting embankments on soft soils in countries like Japan, Sweden, and the United Kingdom. Several case histories are reported in literature regarding the successful use of DMC columns for improving soft ground.

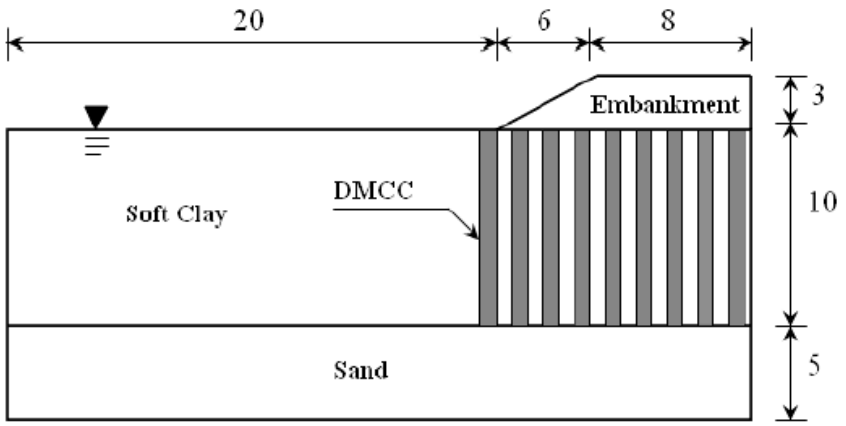

Figure 4.18: Half section view of embankment on soil mixing columns (all dimensions in meters)

A study conducted in Kerala (India) from the Indian Institute of Science [24] investigated the performance of embankments founded on organic clay stratum reinforced with deep mixed columns. The soft organic clay considered has a very low shear strength and high compressibility. The in-situ water content of the clay ranges from 100 to 200 %, almost equal to or more than its liquid limit.Ground improvement with in situ deep mixed cement columns has advantages of acceler-

ated construction and reduced settlements and is a promising technique that can be used for improving this type of clay.
In this study a numerical analysis was conducted and the model geometry considered is shown on figure 4.18.

The results show that there is an increase of the Factor of Safety with the inclusion of soilcrete : the FS of the embankment founded on the in situ soil without soilcrete columns was 0.98 columns, after the reinforcement with columns with a higher water cement ratio (W/C)of 6.5, the FS increases to 1.07.

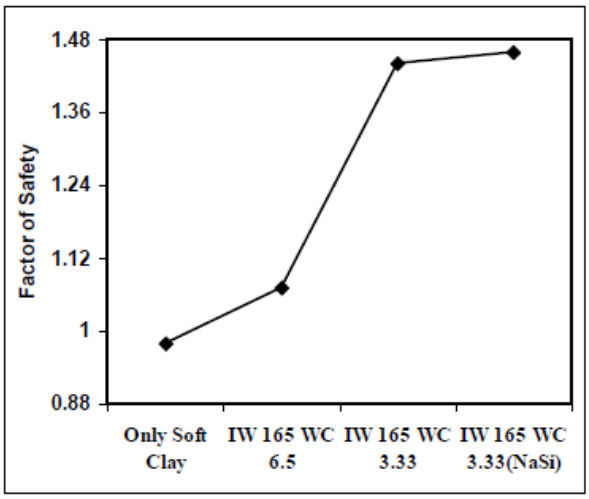

Figure 4.19: Influence of column properties on Factor of Safety

So the Indian Institute of Science, through a numerical analysis, demonstrated that the provision of soilcrete columns is found to be effective in improving the overall performance of the foundation for embankment construction in terms of settlement and Factor of safety. The second interesting aspect is that with reduction in water cement ratio of the columns inclusions it was found that the stability and settlement characteristics of the embankment foundation system improved, for a given column spacing and area.

4.2 Soil Mix Technology for Remediation and Ground Improvement

The theme of environmental remediation of contaminated sites, such as disused landfills or former industrial sites, represents a complex environmental problem. Contaminated land remediation using soil mix technology is a cost effective and versatile approach with numerous environmental advantages. Further commercial advantages can be realised by combining this with ground improvement which is the core objective of Deep Mixing Method. Also this technique can be useful in the event of complications related to remediation projects of an area (for example due to risks associated to excavation and transport operations, i.e when the level of contamination makes the procedure inapplicable or costs would simply be too high), so a possible alternative consists in securing the contaminated area using a confinement facility. One of the most popular procedure for confinement of contaminated zones is belting with vertical diaphragms in order to prevent and delimit the diffusion of contaminants in the ground. In-situ remediation of contaminated land can need low permeability containment walls, that are cut-off low permeability walls designed to isolate a contaminated area from the surrounding environment.

Project SMiRT is the largest research and development funded project to date by the UK Technology Strategy Board on Contaminated Land Remediation Technologies. It is led by Eco Foundations and involved the collaboration with Cambridge University and 17 industrial partners and is a four year project which commenced in October 2007. Project SMiRT aimed to achieve significant technical advancement and cost-savings by developing innovative SMT systems for integrated remediation and ground improvement, with simultaneous delivery of wet and dry additives, and with advanced quality assurance system. A paper [25] was published in order to present details of the design and execution of the field trials which initial field testing which followed and which took place in the summer of 2011 and to highlight site and project specific issues related to the use of Soil Mix Technology for integrated remediation and ground improvement (4.20).

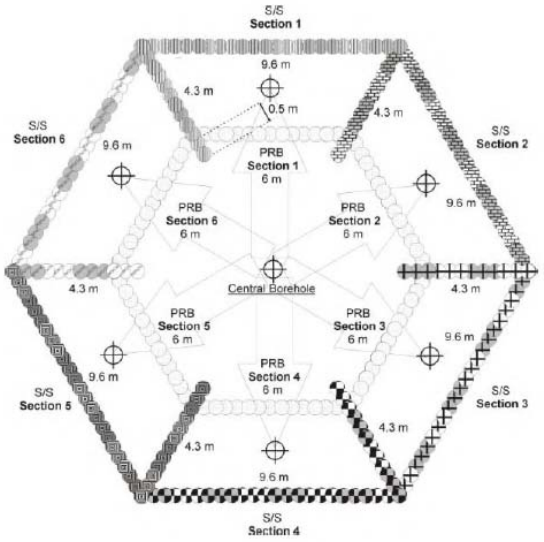

(a) *Schematic of the hexagon of inner PRB walls and outer low permeability walls*

(b) *Image of the hexagon*

Figure 4.20: Schematic of the hexagon

This study involves the use of mixing tools and additives to construct permeable reactive in-ground barriers and low-permeability containment walls and soil treatment by stabilisation/solidification. Permeable reactive barriers (PRBs) are permeable walls installed in the ground to intersect the flow of contaminated groundwater. Reactive material placed in the barrier is designed to remove the contaminants by one of more processes including absorption, precipitation, oxidation, biodegradation and encapsulation. Low permeability containment walls are cut-off low permeability walls designed to isolate a contaminated area from the surrounding environment. Stabilisation/ solidification (S/S) treatments include the physical encapsulation and chemical fixation of contaminants in place

through a range of processes including sorption, precipitation, lattice incorporation, complexation and encapsulation.
The use of soilcrete walls as a remediation technique is useful to limit damages from a contamination of a specific area; at the same time, however, it is a passive measure and does not provides for the removal of contaminants. That's why this method is applied with other procedures, such as permeable reactive barriers to reduce and remove the pollutants from the ground.

4.3 Soil Mix Walls as retaining structures

In recent years, soil mix walls (SMW) have become an economical alternative to traditional excavation support systems. As example of soil mixing technique applied for earth retaining solution is presented in the case of the the construction of the underground floors of "Hotel Montaigne" building, located at Cannes, France [26]. Considering the geological and geotechnical constraints, the presence of high water table and the surrounding conditions near existing buildings, it was performed a retaining wall of soil-cement panels executed using the deep soil mixing technology, in particular the Cutter Soil Mixing (CSM) technology. The existing hotel was remodelled and expanded, with the construction of an additional high floor in the existing building and a new building block with seven floors high and three underground floors and the retaining wall was designed to allow the excavation of the underground floors of the new building block. The execution process started with the execution of the CSM panels before the excavation.

Figure 4.21: View of the work after the execution of CSM

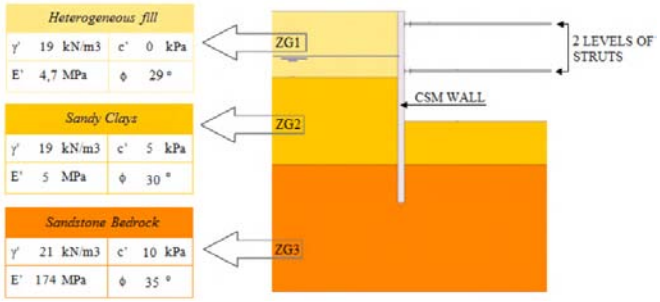

Figure 4.22: Main Geotechnical parameters and representation of a cross-section of the excavation

The execution of the Cutter Soil Mixing retaining wall for the excavation of the new building block of "Hotel Montaigne" constituted an appropriate option with technical, economic and environmental advantages.
The main objective of ensuring the minimization of interferences in the surrounding area was achieved with the CSM retaining wall. During the excavation, the CSM panels allowed also the reduction of the water inflow to the interior of the excavation. The study demonstrated that during the excavation occur low displacements of the retaining wall and that shows the excellent performance of the adopted solution.

Conclusions

The *Deep Soil Mixing* has became a technique that finds different fields of application; such as retaining walls, soil stabilisation, soil remediation, foundation, water shield. In recent years, the use of this methodology for implementing different soil stabilisation configurations is emerging, considering the many advantages offered and compared with the other available, such as high productivity and limited production of waste material and economic benefits.The objective of this study at the laboratory L2MGC of the University of Cergy-Pontoise was to contribute to the understanding of the soil mix material in order to optimise the design of structures, evaluating different aspects related to mixing methods and parameters, exposure conditions and how the mechanical and physical properties are affected.

The first chapter and second chapter include the bibliographical research and the experimental investigation. Tests were carried out to characterise the soil before adding the cementitious binder, the soil-concrete characteristics (compressive strength, dynamic and static modulus of elasticity) at room temperature (20 °C) and in function of the time, then test on soil mix material durability (carbonation and sulphate attacks) and the behavior at high temperature has been investigate after heating until 200,300,600 and 850 °C.

The experimental results are described in the last chapter:

Physical and mechanical properties The main soil used is a silty clay with a liquid limit of 46.8 % and a plastic limit of 18 %. The mixtures with cement are created in order to keep a constant value of the water content of 50 % and the dosage in cement ranges from 150 to 300 kg/m^3. The permeability ranges from $1.4 \cdot 10^{-11}$ to $9.4 \cdot 10^{-10}$. After 180 days of curing time there is an increase in the compressive strength, dynamic modulus of elasticity and wave speed P with a

logarithmic function. The mechanical properties grow with cement dosage. The deformability increases when the dosage of cement is lower.

Sulphate attacks The consequence of the formation of ettringite and gypsum in the soil mix material is its swelling resulting in crack formation and leads to a gain in mass and a loss of compressive strength.The change in wave speed P values compared to regular specimens without sulphate inside is not significant.

Carbonation The results from the carbonation study have shown that the carbonation phenomena are higher with soil-cement mixture than to conventional concretes. This explained by the nature of the cement, CEM III C that is a slag cement, the high porosity and permeability and the low cement content. By increasing the cement content, the carbonation resistance is enhanced. Specimens with a higher water content are less subject to carbonation and in general a high level of relative humidity enhance the process of carbonation.

Behavior at high temperature The TG and TD analyses highlight the decomposition of gypsum, dehydration of C-S-H, dehydroxylation of clay and the decomposition of $CaCO_3$. The behavior at high temperature of the soil indicates that the kind of clay is a *Montmorillonite*. The thermal response shows the mass loss of water and the large amount of free water drives,under heating, a significant drop in temperature between the core and surface temperature of the specimens. The loss mass is related to the initial water content of the specimens. The results are consistent with the evolution of the mechanical properties as a function of temperature and with the cracks observation. After 850 °C the material loses all its mechanical resistance.

The last chapter highlights some applications of Deep Mixing Method in order to demonstrate how the technique can improve in general the stability and safety of earth structures. In particular the examples are focused on the stability of embankment, investigated through simulations with software *Geostudio* after the introduction of soilcrete walls into the levee as reinforcement; then there are some case studies that show how soil mixing material can be used for remediation of contaminated soils and as retaining structures. All of this examples demonstrate the effectiveness of the technique.

Prospects In this study the amount of water in the mixtures was set. The study may be further developed for a different W/C ratio in order to optimize

the physical and mechanical properties, especially under heating since these properties are already strongly affected after a heating history of 200 °C. Due the large amount of water and the kind of clay (Montmorillonite), with its high specific surface, the W/C can be optimized.

Durability of soil cement material was investigated for a period too short (six months) to give a complete explanation of the phenomenon. Normally these tests are performed for a longer period of time (one year or more) because the long-term properties take a much longer period to develop and small changes are still occurring after several years.

Bibliography

[1] Bruce, M. E. C., Berg, R. R., Collin, J. G., Filz, G. M., Terashi, M., Yang, D. S., & Geotechnica, S. (2013). *Federal Highway Administration design manual: Deep mixing for embankment and foundation support* . United States. Federal Highway Administation. Offices of Research and Development.

[2] Hussin, J. D. (2006). *Methods of soft ground improvement.* The Foundation Engineering Handbook, 529-565.

[3] Guggenheim, S., Brady, J., Mogk, D., & Perkins, D. (1977). *Introduction to the properties of clay minerals.* Mineralogical Society of America, Washington, DC.

[4] Szymkiewicz, F., Barrett, A. G., Marino, J. P., Le Kouby, A., & Reiffsteck, P. (2015, June). *Assessment of strength and other mechanical properties of the Deep Mixing material.*

[5] Osmanovic, Z., Haračić, N., & Zelić, J. (2018). *Properties of blastfurnace cements (CEM III/A, B, C) based on Portland cement clinker, blastfurnace slag and cement kiln dusts.* Cement and Concrete Composites, 91, 189-197.

[6] Irassar, E. F., Di Maio, A., & Batic, O. R. (1996). *Sulfate attack on concrete with mineral admixtures.* Cement and Concrete Research, 26(1), 113-123.

[7] Al-Amoudi, O. S. B. (2002). *Attack on plain and blended cements exposed to aggressive sulfate environments.* Cement and Concrete Composites, 24(3-4), 305-316.

[8] J. Prasad,D.K. Jain and A.K. Ahuja ,(2006), *Factors influencing the sulphate resistance of cement concrete and mortar*,Department of Civil Engineering, I.I.T.R., Roorkee, India

[9] Nakarai, K., & Yoshida, T. (2015). *Effect of carbonation on strength development of cement-treated Toyoura silica sand.* Soils and Foundations, 55(4), 857-865.

[10] Ho, L. S., Nakarai, K., Ogawa, Y., Sasaki, T., & Morioka, M. (2017). *Strength development of cement-treated soils: Effects of water content, carbonation, and pozzolanic reaction under drying curing condition.* Construction and Building Materials, 134, 703-712.

[11] I. Marzano, (2009),*La tecnica del Soil Mixing per la cinturazione di siti contaminati*

[12] Sharma, N. K., Swain, S. K., & Sahoo, U. C. (2012). *Stabilization of a clayey soil with fly ash and lime: a micro level investigation.* Geotechnical and geological engineering, 30(5), 1197-1205.

[13] Millogo, Y., Morel, J. C., Traoré, K., & Ouedraogo, R. (2012). *Microstructure, geotechnical and mechanical characteristics of quicklime-lateritic gravels mixtures used in road construction.* Construction and Building Materials, 26(1), 663-669.

[14] Peethamparan, S., Olek, J., & Diamond, S. (2009). *Mechanism of stabilization of Na-montmorillonite clay with cement kiln dust.* Cement and Concrete research, 39(7), 580-589.

[15] Földvári, M. (2011). *Handbook of thermogravimetric system of minerals and its use in geological practice* (Vol. 213, pp. 1-180). Budapest: Geological Institute of Hungary.

[16] Laneyrie, C., Beaucour, A. L., Green, M. F., Hebert, R. L., Ledesert, B., & Noumowe, A. (2016). *Influence of recycled coarse aggregates on normal and high performance concrete subjected to elevated temperatures.* Construction and Building Materials, 111, 368-378.

[17] Helson, O. (2017). *Comportement thermo-hydro-mécanique et durabilité des bétons de sol: influence des paramètres de formulation et conditions d'exposition* ,Doctoral dissertation, University of Cergy-Pontoise.

[18] Accornero, N. (2018). *IL FENOMENO DELLO SPACCO ESPLOSIVO-Come il rapporto acqua/legante, la percentuale dei vuoti d'aria e il contenuto di fibre influenzano il comportamento del calcestruzzo indurito soggetto ad elevate temperature.= THE PHENOMENON OF EXPLOSIVE SPALLING-How the water/binder ratio, percentage of air voids and fiber content affect the performances of hardened concrete subjected to elevated temperatures* Doctoral dissertation, Politecnico di Torino.

[19] Xing, Z. (2011). *Influence de la nature minéralogie des granulats sur leur comportement et celui des bétons à hautes températures.* Laboratoire de Mécanique et Matériaux du Génie Civil. Thèse de doctorat en génie civil, Université de Cergy-Pontoise.

[20] Fan, J., Wang, D., & Qian, D. (2018). *Soil-cement mixture properties and design considerations for reinforced excavation.* Journal of Rock Mechanics and Geotechnical Engineering, 10(4), 791-797.

[21] Balmer, G. Glenn. (1958). *Shear strength and elastic properties of soil-cement mixtures under triaxial loading*

[22] Aydogmus, T., Alexiew, D., & Klapperich, H. (2004, March). Investigation of interaction behaviour of cement-stabilized cohesive soil and PVA geogrids. In Geotechnical engineering with geosynthetics, Proceedings of the third European Geosynthetics Conference, Munich, Germany. p (Vol. 3).

[23] Mitchell, J. K. (1976). *The properties of cement-stabilized soils.* In Proceeding Residental Workshop on Materials and Methods for Low Cost Road, Rail and Reclamation Works, Leura, Australia.

[24] Suganya, K., & Sivapullaiah, P. V. (2012). *Parametric study of embankments founded on soft organic clay using numerical simulations.* In ISSMGE—TC 211 international symposium on ground improvement IS-GI Brussels (Vol. 31).

[25] Al-Tabbaa, Abir & Liska, Martin & Ouellet-Plamondon, Claudiane & Jegandan, S. & Shrestha, R. & Barker, P. & McGall, R. & Critchlow, C.. (2012). *Soil Mix Technology for Integrated Remediation and Ground Improvement: From Laboratory Work to Field Trials.* Geotechnical Special Publication. 522-532.

[26] Peixoto, Artur. (2012). *Permanent Excavation Support in Urban Area using Cutter Soil Mixing technology at Cannes*, France.

Remerciements

Je voudrais remercier toute l'équipe de l'Université de Cergy-Pontoise avec Anne-Lise Beaucour, Javad Eslami, Prosper Pliya et Albert Noumowe de m'avoir accueilli et permis de faire cette expérience auprès du laboratoire L2GMC. Je remercie aussi Jacques Hessouh avec lequel j'ai pu travailler et apprendre. Je remercie tout le monde pour la disponibilité et d'avoir été suivie dans ce travail pour la période de stage.

Ringraziamenti

Desidero innanzitutto ringraziare il Professore Paolo Simonini e la Professoressa Anne-Lise Beaucour per avermi permesso di svolgere questa esperienza in Francia.In secondo luogo desidero ringraziare i miei genitori per avermi sostenuto da sempre in tutte le mie scelte, ed in particolare durante il mio percorso universitario. Desidero inoltre ringraziare tutte le persone che mi sono state vicine, i miei amici e la mia famiglia, insieme ai colleghi dell'Università di Padova e dell'Université de Cergy Paris. Infine desidero ringraziare la Professoressa Anne-Lise Beaucour per avermi accolto nel laboratorio L2MGC dell'Université de Cergy Paris e per avermi seguita nel lavoro di ricerca assieme a Jacques Hessouh.

Grazie a tutti,
Sara